2.2 Solar System Abundances of the Elements

H Palme, Forschungsinstitut und Naturmuseum Senckenberg, Frankfurt am Main, Germany
K Lodders, Washington University, Saint Louis, MO, USA,
A Jones, Université Paris Sud, Orsay Cedex, France

This article is a revision of the previous edition article by H. Palme and A. Jones, volume 1, pp. 41–61, © 2003, Elsevier Ltd.

2.2.1 Abundances of the Elements in the Solar Nebula

2.2.1.1 Historical Remarks

At the beginning of the twentieth century, the first mature stage was reached in defining the average composition of cosmic matter using reliable compositional data of the Earth's crust and meteorites. A detailed account of the search for the 'cosmic' inventory of the chemical elements can be found in Lodders and Fegley (2011), and the historical excursion is restricted to a few highlights here. Harkins (1917) discovered that elements with even atomic numbers are more abundant than those with odd atomic numbers. This Oddo–Harkins rule is best exemplified for the rare earth elements (REE). During the 1920s and 1930s, Victor Moritz Goldschmidt and his colleagues in Göttingen, and later in Oslo, measured and compiled a wealth of chemical data on terrestrial rocks and meteorites, including individual phases of meteorites. Goldschmidt (1938) used these data to devise a cosmic abundance table, which he published in 1938 in the ninth volume of his 'Geochemische Verteilungsgesetze der Elemente' (The Geochemical Laws of the Distribution of the Elements) under 'Die Mengenverhältnisse der Elemente und der Atom-Arten' (The proportions of the elements and the various kinds of atoms). Goldschmidt believed that meteorites would provide the average composition of cosmic matter. He used the word 'cosmic' because, like his contemporaneous astronomers, he thought that meteorites represent interstellar matter from outside the solar system. In his book, he gave a second reason for using meteorite data. Most meteorites should be representative of the average cosmic matter because meteorites as a whole have not been affected by physical and/or chemical processes (e.g., melting and crystallization), even if individual components such as chondrules within meteorites are products of melting and crystallization processes before the meteorites assembled. In contrast to undifferentiated meteorites, the crust of the Earth formed by melting of mantle rocks that then separated from the mantle and therefore the crust can only provide a very biased sampling of elemental abundances in the bulk Earth. Goldschmidt calculated the average concentrations of elements in cosmic matter from a weighted mean of the element abundances in meteorite phases: metal (two parts), sulfide (one part), and silicates (ten parts). In this way, he obtained the cosmic abundances of 66 elements.

At about the same time, astronomers succeeded in quantifying elemental abundances in the solar photosphere from absorption spectroscopy. It was soon realized that the composition of

the Sun and the whole Earth is similar, except for hydrogen and the extremely volatile elements (see Russell, 1929).

Almost 20 years after Goldschmidt, Suess and Urey (1956) published a new abundance table, which in part relied on solar abundances. Suess and Urey (1956) introduced constraints on elemental abundances from nucleosynthesis. Their semiempirical abundance rules primarily describing the smooth abundance variation of odd-mass nuclei with increasing mass number were applied to estimate the abundances of the elements for which analytical data from meteorites were not available or had large errors. The Suess and Urey compilation was influential for theories of nucleosynthesis and for the development of nuclear astrophysics in general. Later compilations by Cameron (1973), Anders and Grevesse (1989), Palme and Beer (1993), Lodders (2003), and others took into account improved analytical data on meteorites and the more accurate determination of elemental abundances in the solar photosphere. There has been a continuous convergence of abundances derived from meteorites and those obtained from solar absorption line spectroscopy. The agreement is now better than ±10% for most elements, as described in the succeeding text.

2.2.1.2 Solar System Abundances of the Elements

2.2.1.2.1 Is the solar nebula compositionally uniform?

Until the 1970s, it was often assumed that the Sun, the planets, and all other objects of the solar system formed from a gaseous nebula with well-defined chemical and isotopic composition. The discovery of comparatively large and widespread variations in oxygen isotopic compositions has cast doubt upon this assumption (see Begemann, 1980, and references therein). The evidence for incomplete mixing and homogenization in the primordial solar nebula was provided by isotopic anomalies for a variety of elements in refractory inclusions of carbonaceous chondrites. The discovery of genuine stardust corroborated the conclusion that the solar nebula was not well mixed. The micrometer-size (or less) 'presolar' grains of mainly silicon carbide, nanodiamond, graphite, corundum, spinel, and silicate grains are embedded in meteorites and are detected and characterized by their huge isotope anomalies in carbon, nitrogen, oxygen, silicon, and some heavy elements (see reviews by, e.g., Lodders and Amari (2005); **Chapter 1.4**). Since the first edition of the *Treatise in Geochemistry* in 2003, a wealth of new data has appeared about the isotopic composition of heavy elements in planets and in meteorites and their components.

Aside from oxygen, the three most abundant heavy elements silicon, magnesium, and iron are isotopically uniform in solar system materials (except for small mass-dependent fractionations during physical and chemical processes such as diffusion). The difference in silicon isotopic composition observed in Earth compared to meteorites is ascribed to fractionation of silicon isotopes during partitioning of silicon into core-forming metal (e.g., Armytage et al., 2011, and references therein).

However, in meteorites, other minor and trace elements show significant isotopic variations that must be ascribed to addition or loss of nucleosynthetic components, such *r*-process or *s*-process nuclei. For example, there are ubiquitous variations in neutron-rich isotopes of extraterrestrial samples (e.g., ^{48}Ca, ^{50}Ti, ^{54}Cr, ^{58}Ni, ^{62}Ni, and ^{64}Ni). An example is given in **Figure 1** where Δ^{17}O is plotted against ε^{54}Cr for a variety of solar system materials (Warren, 2011). The variations in

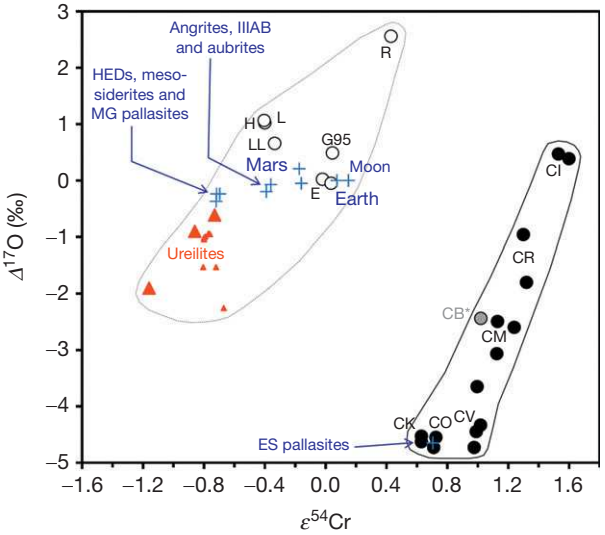

Figure 1 A plot of Δ^{17}O (deviation from the terrestrial fractionation line in a δ^{17}O vs. δ^{18}O plot, in ‰) plotted against ε^{54}Cr (deviation from terrestrial ^{54}Cr/^{52}Cr in parts per ten thousand) demonstrates the isotopic nonuniformity of solar system materials. A similar variability is seen for the neutron-rich isotopes of titanium and nickel. Carbonaceous chondrites are clearly separated from other chondrite types and the planets. The difference between main group (MG) and Eagle Station (ES) pallasites seems to indicate two different parent bodies for pallasites. The figure is taken from Warren PH (2011) Stable-isotopic anomalies and the accretionary assemblage of the Earth and Mars: A subordinate role for carbonaceous chondrites. *Earth and Planetary Science Letters* 311: 93–100.

oxygen isotopes have a different origin than those of chromium isotopes. **Figure 1** illustrates that two groups, carbonaceous and noncarbonaceous materials, are well separated in both isotopes, but the reason is unclear. This shows that the solar system is not uniform in isotopic composition although the variations are very small. The variations in ^{54}Cr/^{52}Cr are about 1 part in 10 000. For oxygen isotopes, variability is larger and often given as deviation from the terrestrial fractionation line (TF) in the δ notation, indicating changes in isotope ratios of 1 part per 1000 (Clayton, 1993).

A nucleosynthetic origin of the observed variations in oxygen isotopes is now viewed as unlikely, but cannot be ruled out. The currently widely favored model is self-shielding (Clayton, 2002). The isotopic variations seen in **Figure 1** may be produced by the presence of small and extremely ^{54}Cr-enriched grains. The observed variations in chromium may be due to the variable addition of ^{54}Cr-rich nanoparticles (Dauphas et al., 2010; Qin et al., 2011). The differences in oxygen and chromium isotopes between the main group and Eagle Station pallasites (**Figure 1**) demonstrate that chemically and structurally identical meteorites may have different stable isotopic compositions and may thus come from different parent bodies with similar evolution.

Although isotopic deviations from terrestrial standards ('isotope anomalies') in solar system materials are widespread, they are generally far below 1%. It is still a plausible working hypothesis that the bulk of the matter in the primordial solar nebula from which the solar system formed was relatively uniform in chemical and isotopic composition. The elemental composition of the solar system is roughly similar to that of

many other stars in the solar neighborhood. However, there are compositional differences among stars that are at similar stages of stellar evolution (e.g., dwarf stars). Their variability in heavy element content is not caused by nucleosynthesis in the stars themselves but rather reflects galactic chemical evolution. Nucleosynthesis in previous generations of stars led to heavy element enrichment of the interstellar medium (ISM) over time, and newly formed stars inherited the heavy elements that were available at the place and time when they formed. There are also truly exotic stars that make the term 'cosmic abundances of elements' questionable. Therefore, the authors use the term 'solar system abundances' or 'solar abundances' of the elements and avoid the term 'cosmic abundances.'

2.2.1.2.2 The composition of the solar photosphere

The determination of the elemental abundances in the Sun is possible through quantitative analysis of absorption lines of the solar photosphere. Although this provides only data for the composition of the outer few hundred kilometers, the photosphere is thought to be chemically representative of the bulk Sun, because of convection and mixing in the Sun. Present models of the Sun assume gravitational settling of heavier elements from the photosphere to the interior of the Sun over the lifetime of the Sun, leading to a continuous depletion of helium and other heavy elements relative to the dominant hydrogen. But the relative abundances of heavy elements are assumed not to be affected significantly by this process (e.g., Lodders et al., 2009; Piersanti et al., 2007).

The quantitative determination of photospheric abundances involves three steps: first, the construction of a numerical model atmosphere; then, the calculation of an emitted spectrum based on the model atmosphere; and, finally, a comparison of this spectrum with the observed spectrum (Cowley, 1995). Another assumption usually made in calculating solar abundances is that of local thermodynamic equilibrium (LTE), that is, "the quantum-mechanical states of atoms, ions, and molecules are populated according to the relations of Boltzmann and Saha, valid strictly in thermodynamic equilibrium" (Holweger, 2001). The assumption of LTE may not be justified for a highly inhomogeneous and dynamic plasma permeated by an intense, anisotropic radiation. Newer calculations take effects of NLTE (nonlocal thermodynamic equilibrium) into account. More recent hydrodynamic models include 3D effects such as convective flows and granulation of the solar atmosphere. It is unclear if 3D models produce more accurate solar abundances (see succeeding text), in particular since application of 3D models give rather different abundances for carbon, oxygen, and some other elements depending on the author (Asplund et al., 2009; Caffau et al., 2011a).

Other important factors in the improvements of accuracy of solar abundance determinations are transition probabilities and lifetimes determined in laboratory experiments (Grevesse and Sauval, 1998; see also Sneden et al., 2009, and the references to papers by Lawler therein). New measurements of transition probabilities and lifetimes are an ongoing and active research area because elemental abundance determinations in low-metallicity stars are currently a large research theme in astronomy. Thus, one can expect that solar abundance determinations will become even more accurate in the future.

Table 1 lists the composition of the solar photosphere from absorption spectroscopy. Abundances are normalized to 10^{12} hydrogen atoms on a logarithmic scale that is usually used in astronomy. The data are from a recent compilation by Lodders et al. (2009) with some updates described later. The reader is referred to this paper for an explanation and sources of the individual elemental abundances. Solar abundances for which updates (2009) are included are marked 'c' in column 5 of Table 1, and comments are given in the succeeding text. All updates are minor. The comparison to meteorite data in Table 1 is taken from a later section, but the authors note that the accuracy and precision of the solar abundances based on absorption line spectroscopy are approaching those of the meteorite data.

The following changes were made to the previous table (Lodders et al., 2009).

Lithium. The new value is from Caffau et al. (2011a). Lithium in meteorites is still two orders of magnitude higher than in the Sun because lithium is destroyed in the Sun. Note that beryllium has comparable abundances in meteorites and the Sun.

Carbon. The new carbon value of Caffau et al. (2010) is about 30% higher. The C/O ratio is 0.59 instead of 0.46 in Lodders et al. (2009).

Nitrogen. The nitrogen value is the same as in Lodders et al. (2009) but based on Caffau et al. (2009).

Oxygen. No changes were made to the value of 8.73 ± 0.07 recommended in Lodders et al. (2009). This value is based on the average from three determinations by Melendez and Asplund (2008), Caffau et al. (2008), and Ludwig and Steffen (2008). Another compilation by Asplund et al. (2009) suggests 8.70 ± 0.05. Note that the solar oxygen abundance remains uncertain.

Sulfur. The new value of Caffau et al. (2011a) is only a small change from Lodders et al. (2009).

Potassium. The new value of Caffau et al. (2011a) differs little from the value given by Lodders et al. (2009), but the uncertainty has grown.

Iron. The value selected in Lodders et al. (2009) was adopted from the compilation of Lodders (2003) as 7.45 ± 0.08. Melendez and Barbuy (2009) presented a new set of oscillator strengths and found 7.45 ± 0.02 from analysis of Fe II lines and various model atmospheres, which is consistent with the previous value but with a smaller uncertainty. Using the gf factors from Melendez and Barbuy (2009), Mashonkina et al. (2011) determined 7.47 ± 0.05 for 1D models but a range of 7.41 ± 0.11 to 7.56 ± 0.05 depending on the gf source. Also using gf factors from Melendez and Barbuy (2009), Caffau et al. (2011a) find 7.51 ± 0.06 from Fe II lines when they apply their 3D model. Caffau et al. (2011a) investigated the effect of using disc center and integrated disc spectra, line selections, and other gf values on the results and recommend 7.52 ± 0.06 as their preferred value. Asplund et al. (2009) recommend 7.50 ± 0.04 from their 3D models and the use of the transition probabilities from Melendez and Barbuy (2009). The average of the four determinations with the same gf values but different models (7.45, 7.47, 7.51, and 7.50) leads to 7.48 with a conservative uncertainty estimate of 0.06.

Zirconium. The new value from Caffau et al. (2011b) has increased by ~10% from the value given by Lodders et al. (2009), and the uncertainty is larger.

Table 1 Solar photospheric abundances and meteorite-derived solar system abundances (log abundance $A(H) = 12$)

		Solar photosphere	*s.d. (dex)*	*com*	*Meteorite (CI)*	*s.d. (dex)*	*Sun/meteorite (N_{sun}/N_{met})*
1	H	12			8.24	0.04	5.70×10^3
2	He	10.925	0.02		1.31		4.09×10^9
3	Li	1.03	0.03	c	3.27	0.04	0.01
4	Be	1.38	0.09		1.34	0.03	1.10
5	B	2.70	0.17		2.81	0.04	0.78
6	C	8.50	0.06	c	7.42	0.04	12.0
7	N	7.86	0.12	c	6.28	0.06	38.30
8	O	8.73	0.07	c	8.41	0.04	2.08
9	F	4.56	0.30		4.44	0.06	1.32
10	Ne	8.05	0.10		−1.10		1.40×10^9
11	Na	6.30	0.03		6.29	0.04	1.03
12	Mg	7.54	0.06		7.55	0.02	0.98
13	Al	6.47	0.07		6.45	0.03	1.06
14	Si	7.52	0.06		7.53	0.01	0.97
15	P	5.46	0.04		5.46	0.03	1.01
16	S	7.16	0.05	c	7.18	0.02	0.96
17	Cl	5.50	0.30		5.25	0.06	1.79
18	Ar	6.50	0.10		−0.48		9.60×10^6
19	K	5.11	0.09	c	5.10	0.04	1.03
20	Ca	6.33	0.07		6.31	0.03	1.05
21	Sc	3.10	0.10		3.06	0.03	1.08
22	Ti	4.90	0.06		4.92	0.03	0.95
23	V	4.00	0.02		3.98	0.03	1.04
24	Cr	5.64	0.01		5.66	0.02	0.96
25	Mn	5.37	0.05		5.50	0.03	0.75
26	Fe	7.48	0.06	c	7.48	0.02	1.00
27	Co	4.92	0.08		4.89	0.02	1.06
28	Ni	6.23	0.04		6.22	0.03	1.02
29	Cu	4.21	0.04		4.27	0.06	0.86
30	Zn	4.62	0.15		4.63	0.02	0.98
31	Ga	2.88	0.10		3.09	0.03	0.61
32	Ge	3.58	0.05		3.61	0.04	0.94
33	As				2.32	0.04	
34	Se				3.36	0.03	
35	Br				2.56	0.06	
36	Kr	3.28	0.08		−2.25		3.41×10^5
37	Rb	2.60	0.10		2.39	0.03	1.63
38	Sr	2.92	0.05		2.90	0.03	1.04
39	Y	2.21	0.02		2.17	0.02	1.10
40	Zr	2.62	0.06	c	2.55	0.02	1.17
41	Nb	1.44	0.06	c	1.44	0.04	1.01
42	Mo	1.92	0.05		1.95	0.04	0.92
44	Ru	1.84	0.07		1.79	0.02	1.13
45	Rh	1.12	0.12		1.06	0.02	1.14
46	Pd	1.66	0.04		1.67	0.02	0.97
47	Ag	0.94	0.30		1.22	0.04	0.52
48	Cd	1.77	0.11		1.73	0.03	1.09
49	In	1.50	ul		0.78	0.02	5.97
50	Sn	2.00	0.30		2.09	0.06	0.81
51	Sb	1.00	0.30		1.03	0.06	0.94
52	Te				2.21	0.03	0.01
53	I				1.57	0.08	0.03
54	Xe	2.27	0.08		−1.92		1.56×10^4
55	Cs				1.10	0.03	0.08
56	Ba	2.2	0.1		2.20	0.02	1.00
57	La	1.14	0.03	c	1.19	0.01	0.88
58	Ce	1.61	0.06	c	1.60	0.01	1.03
59	Pr	0.76	0.04	c	0.78	0.01	0.96
60	Nd	1.45	0.05	c	1.47	0.01	0.96
62	Sm	1.00	0.05	c	0.96	0.01	1.09
63	Eu	0.52	0.02	c	0.54	0.01	0.95
64	Gd	1.11	0.05	c	1.07	0.01	1.09

(*Continued*)

Table 1 (Continued)

		Solar photosphere	*s.d. (dex)*	*com*	*Meteorite (CI)*	*s.d. (dex)*	*Sun/meteorite (N_{sun}/N_{met})*
65	Tb	0.28	0.05	c	0.33	0.01	0.89
66	Dy	1.13	0.06	c	1.15	0.01	0.95
67	Ho	0.51	0.10	c	0.49	0.01	1.05
68	Er	0.96	0.05	c	0.95	0.01	1.03
69	Tm	0.14	0.04	c	0.14	0.01	1.00
70	Yb	0.86	0.10	c	0.94	0.01	0.83
71	Lu	0.12	0.08	c	0.11	0.01	1.03
72	Hf	0.88	0.05		0.73	0.01	1.42
73	Ta				−0.13	0.04	1.34
74	W	1.11	0.15		0.67	0.04	2.75
75	Re				0.29	0.02	0.52
76	Os	1.36	0.19	c	1.37	0.02	0.85
77	Ir	1.38	0.05		1.34	0.02	1.09
78	Pt	1.74	0.30		1.63	0.02	1.29
79	Au	1.01	0.18		0.83	0.05	1.52
80	Hg				1.20	0.18	0.06
81	Tl	0.95	0.20		0.79	0.05	1.45
82	Pb	2.00	0.06		2.05	0.03	0.88
83	Bi				0.67	0.04	0.21
90	Th	<0.08	ul	c	0.06	0.03	
92	U	<-0.47	ul		−0.52	0.03	

ul, upper limit; c, comment, see text.

Niobium. The new value from Nilsson et al. (2010) is only ~5% higher than the value given by Lodders et al. (2009).

REE. As in Lodders et al. (2009), the REE are largely taken from Sneden et al. (2009).

Osmium. Caffau et al. (2011a) recommend 1.36 ± 0.19, ~20% lower than the value given by Lodders et al. (2009).

Thorium. Caffau et al. (2011a) suggest 0.08 ± 0.03. The authors believe that the uncertainty given by these authors is somewhat optimistic even if a somewhat better fit to the strongly blended thorium line was achieved. Thus, the authors prefer to only recommend an upper limit for the thorium abundance.

A comparison of the photospheric abundances in **Table 1** with a recent compilation by Asplund et al. (2009) shows good agreement between the two data sets. There are 34 elements where the agreement is within 10% and 13 elements where the difference is less than 20%. Error bars are in most cases larger than the differences. One of the few cases where error bars are lower than the difference is sodium where an uncertainty of about 7% is given in **Table 1**, compared to 10% in Asplund et al. (2009), at a difference of 15% between the two data sets. Slightly lower abundances for C, N, and O were derived by Asplund et al. (2009), although the differences between the Aspund et al. (2009) data and the data listed in **Table 1** are in all three cases within error bars. As details of the Asplund et al. (2009) analyses are not yet available, we did not include them in our compilation.

There are no systematic differences between the authors' compilation and the Asplund et al. (2009) data. This is important, as Asplund et al. (2009) have reanalyzed the solar abundances of nearly all available elements, using a new 3D, time-dependent hydrodynamic model of the solar atmosphere, whereas several values in **Table 1** are based on 1D models. However, the important issue of reliable transition probabilities remains as this affects abundance determinations more than the atmospheric model applied (e.g., see notes for the solar iron abundances and the related references).

2.2.1.3 Abundances of Elements in Meteorites

2.2.1.3.1 Differentiated and undifferentiated meteorites

Meteorites fall into two different groups: *undifferentiated* and *differentiated*. Undifferentiated meteorites are pieces of planetesimals that have never been heated to melting temperatures. Their chemical and isotopic composition should be representative of the bulk parent planetesimal. Differentiated meteorites come from planetesimals that were molten and differentiated into the core, mantle, and crust. A meteorite from such a body will not be representative of the bulk planetesimal or planet. It is not a trivial task to derive the bulk composition of the parent body. Undifferentiated meteorites reflect to some degree the composition of the solar nebula from which they formed. Variability in the composition of undifferentiated meteorites reflects inhomogeneity in the solar nebula or disequilibrium during formation of solids from gas or both. A comprehensive discussion of meteorite classification is given by Krot et al. (2003) and **Chapter 1.1**.

2.2.1.3.2 Cosmochemical classification of elements

Many processes responsible for the variable chemical composition of primitive meteorites are related to the formation temperatures of meteoritic components. Although it is difficult to unambiguously prove the condensation origin of a single meteoritic component, the elemental abundance patterns (i.e., the solar-normalized abundances in meteoritic components) suggest that condensation processes must have played an important role in the early solar system. Abundance patterns in chondritic meteorites correlate with condensation

temperatures of the elements in a gas of solar composition assuming thermodynamic equilibrium between solids and gas phase. Major elements condense as minerals, while minor and trace elements condense in solid solution with the major mineral phases. The temperature where half of an element is in the solid phase is called the 50% condensation temperature (Lodders, 2003; Wasson, 1985). Within this framework, five more or less well-characterized components can account for the variations in the elemental abundances in primitive meteorites (**Table 2**). The following components are distinguished by their condensation temperatures:

1. *Refractory elements*. The first phases to condense from a cooling gas of solar composition are calcium, aluminum oxides, and silicates, which can sequester a comparatively large number of trace elements, such as REE, zirconium, hafnium, and scandium. These elements are often named refractory lithophile elements (RLE), in contrast to the refractory siderophile elements (RSE) comprising metals with low vapor pressures, for example, tungsten, osmium, and iridium, which condense as multicomponent metal alloys at similarly high temperatures. On average, the calcium–aluminum-rich inclusions (CAIs) are enriched in both RLE and RSE by a factor of 20 over CI chondrite abundances. The refractory component makes up about 5% of the total condensable matter (Grossman and Larimer, 1974). *Variations in Al/Si, Ca/Si, etc., ratios of bulk chondritic meteorites may be ascribed to the incorporation of variable amounts of early condensed refractory phases.*
2. *Magnesium silicates*. The major fraction of condensable matter is comprised of minerals containing the three most abundant elements heavier than oxygen: silicon, magnesium, and iron. In the reducing environment of the solar nebula, iron condenses almost entirely as metal, while magnesium and silicon form forsterite (Mg_2SiO_4), which, for the most part, is converted to enstatite ($MgSiO_3$) at lower temperatures by reaction with gaseous SiO. Forsterite has an atomic Mg/Si ratio twice the solar system ratio, and loss or gain of the forsterite component is the simplest way to produce variations in Mg/Si ratios. It is also possible that the SiO gas does not fully react with forsterite. This will happen, if the size of the condensed forsterite crystals is large enough to prevent diffusive exchange with the ambient gas. In this case, a high Mg/Si solid mineral assemblage is left as solid nebular condensate (see Petaev and Wood, 1998). *Variations in Mg/Si ratios of bulk meteorites are produced by the incorporation of various amounts of early-formed forsterite and/or incomplete condensation of enstatite.*
3. *Metallic iron* condenses as FeNi alloy at about the same temperature as forsterite, the sequence depending on total pressure. At pressures above 10^{-4} bars, Fe metal condenses before forsterite, and at lower pressures, forsterite condenses ahead of metal (Grossman and Larimer, 1974; Lodders, 2003). *Variations in the concentrations of iron and other siderophile elements in meteorites are produced by the incorporation of variable fractions of metal.*
4. *Moderately volatile elements* have condensation temperatures below magnesium silicates and FeNi but above the condensation temperatures of the highly volatile elements that are incompletely condensed, even in the moist volatile-rich CI chondrites (carbon, nitrogen, oxygen, and the noble gases). The most abundant of the moderately volatile elements is sulfur, which condenses by reaction of gaseous H_2S with solid Fe at 710 K (664 K – 50% T_c), independent of total pressure. The moderately volatile elements may be subdivided in elements condensing between magnesium silicates and troilite (FeS) and elements condensing below troilite. Except for sulfur, moderately volatile elements condense in solid solution with major phases. They are distributed between sulfides, silicates, and metal, depending on their geochemical character. Their normalized abundances in meteorites other than CI chondrites are usually below solar, that is, they have lower element/Si ratios than the Sun or CI chondrites, which is often referred to as these elements being depleted (see succeeding text). **Figure 2** shows abundances of major and moderately volatile elements in CV3 meteorites relative to the same elements in CI meteorites. The depletions of moderately volatile elements correlate with decreasing condensation temperatures but are independent of the geochemical properties of the elements. The group of moderately volatile elements comprises elements with very different geochemical affinity, such as lithophile zinc (in carbonaceous and ordinary chondrites, zinc is mostly in oxides and silicates), chalcophile lead, and the siderophile germanium. The depletion sequence is independent of the geochemical character of the elements, and the *depletions of moderately volatile elements in meteorites are likely produced by incomplete condensation. The amount and the relative abundances of these elements in meteorites are probably the result of removal of volatiles during condensation* (Palme et al., 1988, and references therein).

Table 2 Cosmochemical classification of the elements

Elements	*Lithophile (silicate + oxide)*	*Siderophile + chalcophile (sulfide + metal)*
Refractory component	$T_c = 1850–1355$ K	
	Zr, Hf, Sc, Y, Gd, Tb, Dy, Ho, Er, Tm, Lu, Th, **Al**, U, Nd, Sm, **Ti**, Pr, La, Ta, Nb, **Ca**, Yb, Ce, Sr, Ba, Be, V, Eu	Re, Os, W, Ir, Mo, Ru, Pt, Rh
Main component	$T_c = 1355–1250$ K	
	Mg, **Si**, Cr	**Ni**, Co, **Fe**, Pd
Moderately volatile	$T_c = 1250–252$ K	
Above T_c (S)	Mn, Li, K, P, Na, Cl, B, Rb, Cs, F, Zn, Sn	P, As, Au, Cu, Ag, Sb, Ga, Ge, Bi, Pb, Te, Se, S
Below T_c (S)	Br, I, Tl	Cd, In, Tl, Hg
Highly volatile	$T_c < 250$ K	
	O, N, Xe, Kr, Ar, C, Ne	

Elements in order of decreasing condensation temperatures (T_c) at a pressure of 10^{-4} bar (Lodders, 2003); major elements shown in boldface.

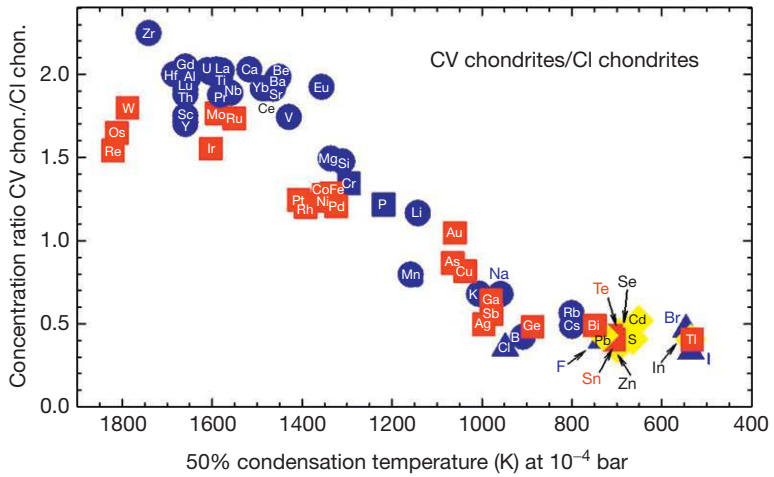

Figure 2 Abundances of elements in CV3 chondrites (e.g., Allende) normalized to CI chondrites are plotted against their 50% condensation temperature. There is a continuous decrease of abundances with increasing volatility as measured by the condensation temperature. The sequence contains elements of very different geochemical character (indicated by different symbol colors: siderophile, red; lithophile, blue; and chalcophile, yellow), indicating that volatility is the only determining parameter in establishing this pattern. Metals with T_c (condensation temperature) above phosphorus are systematically depleted relative to metals with T_c below phosphorus, indicating loss of early-formed metal at temperatures above the T_c of phosphorus. See Palme and Lodders (2009).

5. *Highly volatile elements* that are not fully condensed in CI chondrites have condensation temperatures below that of mercury (see Table 2).

Another important parameter that is often used for distinguishing chondrite groups is oxygen. Both the redox state, expressed as oxygen fugacity, and the oxygen isotopic composition are characteristic properties of individual chondrite groups. The oxygen fugacities recorded in meteoritic minerals cover a wide range, from the high oxygen fugacity recorded by the presence of magnetite in carbonaceous chondrites to the extremely reducing conditions in enstatite chondrites, as indicated by the presence of substantial amounts of metallic silicon dissolved in FeNi. The oxygen fugacity of meteorites is not well defined. Large variations in oxygen fugacity are often recorded among the individual components of a single meteorite. The various components in primitive meteorites apparently represent extreme disequilibrium. Oxygen isotopes give a similar picture (Clayton, 1993). It has been suggested that variations in $\Delta^{17}O$ were produced by reaction of ^{16}O-rich material with a gas rich in ^{17}O and ^{18}O (Clayton, 1993). This gas phase may be considered an additional independent component that contributed to meteorites. *The extent of the gas–solid reactions at various temperatures in the solar nebula and possibly also fluid–solid reactions on a parent body determines the degree of oxidation and the oxygen fugacity of meteoritic components and bulk meteorites.*

2.2.1.4 CI Chondrites as the Standard for Solar Abundances

2.2.1.4.1 Chemical variations among chondritic meteorites

The variations of selected element ratios in different groups of chondritic meteorites are shown in Figure 3. All ratios are normalized to the best estimate of the average solar system ratios from the CI chondrite ratios (taken from Table 3, discussed later). Meteorite groups are arranged in order of decreasing bulk average oxygen contents. Element ratios in the solar photosphere determined by absorption line spectroscopy are shown for comparison (Table 1).

Aluminum is representative of the refractory component in general, and the Al/Si ratios in Figure 3 indicate the level of the refractory component relative to the major fraction of the meteorite (exemplified by the normalization to silicon). The Al/Si ratio of CI chondrites agrees best with the solar ratio, although the ratios in CM chondrites and even ordinary chondrites are almost within uncertainty of the solar ratio. The uncertainties of the meteorite ratios are below 10%, in many cases below 5%. A very similar pattern as for aluminum would be obtained using other refractory elements (calcium, titanium, scandium, REE, etc.), because the ratios of refractory elements in meteorites are constant in all classes of chondritic meteorites, at least within about 5–10% (see, e.g., Pack et al., 2007). The average Sun/CI chondrite ratio of 20 RLE (aluminum, calcium, titanium, vanadium, strontium, yttrium, zirconium, niobium, lanthanum, cerium, praseodymium, neodymium, samarium, europium, gadolinium, terbium, dysprosium, erbium, thulium, and lutetium; see Table 1) is 1.016 with a standard deviation (s.d.) of 0.07. Only elements with an accuracy of the solar abundance determination of better than 25% were included (see Table 1, last column), but hafnium is excluded (see Section 2.2.1.5.1). Elements with larger uncertainties were not considered. The authors conclude that within 5–10% RLE are not fractionated in Orgueil relative to the solar abundances and that the absolute level of refractory elements (relative to silicon) and ratios among refractory elements are the same in CI chondrites and the solar photosphere. The level of refractory elements in other chondritic meteorites (Figure 3) is higher in CM (by 13%) and in CV (by 25%) and lower in H chondrites (by 10%) and enstatite chondrites (by 20%). The agreement between refractory elements in the Sun and in CI chondrites is statistically significant, and all other groups of

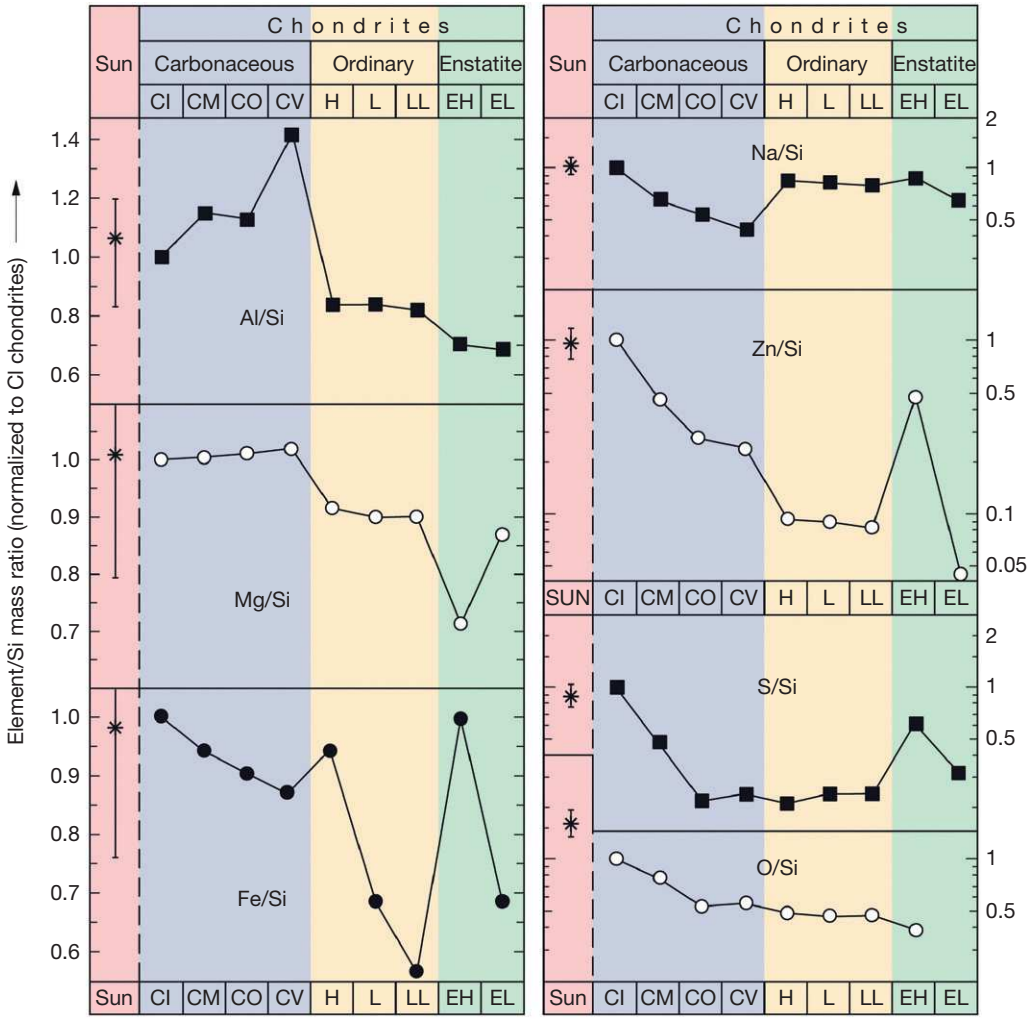

Figure 3 Element/Si ratios of characteristic elements in various groups of chondritic (undifferentiated) meteorites normalized to respective ratios in CI chondrites. Meteorite groups are arranged in order of decreasing oxygen content. The best match between solar photosphere measurements and meteoritic abundances is with CI chondrites (see text for details).

meteorites do not match solar refractory element abundances. The CR chondrites (Renazzo-type meteorites) have CI chondrite ratios of Al/Si (Bischoff et al., 1993) (not shown in **Figure 3**). However, these meteorites are depleted in volatile elements relative to CI chondrites, disqualifying them as a solar system standard. The Mg/Si ratios of CI chondrites also match with the solar abundance ratio (**Figure 3**), but this is less diagnostic because all groups of carbonaceous chondrites have nearly the same Mg/Si ratio (Wolf and Palme, 2001). The ordinary and enstatite chondrites have significantly lower Mg/Si ratios. The error of the solar ratio is about 20% (combining the errors of silicon and magnesium, **Table 1**) and thus spans the range of all classes of chondrites except EH chondrites.

Originally, the known range of the bulk iron contents in chondritic meteorites varied by about a factor of 2, and most meteorite groups are depleted in iron relative to CI chondrites (**Figure 3**). Recently discovered subgroups of carbonaceous chondrites show large excesses of iron (see Krot et al., 2003; **Chapter 1.1**). These CH and CB chondrites suggest that metal behaves as an independent component, and some groups of chondritic meteorites were enriched in iron and other siderophile elements, whereas others were depleted. The excellent agreement of CI chondrite iron abundance with the solar abundance is obvious, although the formal error of the solar Fe/Si ratio is quite large at 20% (**Table 1** and **Figure 3**). However, when considering all siderophile elements, the agreement is much better. The Sun/meteorite abundance ratios of iron, nickel, and cobalt are almost identical. This reduces the uncertainty of the average Sun/meteorite ratio of siderophile elements. Thus only CI and EH chondrites have the solar siderophile/Si ratio (Figure 3). The EH chondrites differ from solar abundances. They are depleted in refractory elements and have fractionated Mg/Si.

In **Figure 3**, the elements sodium, zinc, and sulfur represent the abundances of moderately volatile elements (**Table 2**). Abundance variations are up to a factor of 5 for sulfur and 10 for zinc. All three elements show excellent agreement between the solar and CI chondrite abundances, in contrast to other groups of chondritic meteorites. Enstatite chondrites are an exception in that they nearly reach the level of CI chondrites in their abundances of sodium, zinc, and sulfur. However, enstatite chondrites cannot be representative of solar

Table 3 Solar system abundances based on CI chondrites

		Lodders et al. (2009), updated (1)					*Anders and Grevesse (1989) (2)*		
Element		*Mean CI abundance (by mass)*		*Δ in % relative to (1)*	*Estimated accuracy in (%)*	*Atoms per 10^6 atoms of Si*	*Mean CI abundance (by mass)*		*Atoms per 10^6 atoms of Si*
1	H	1.97	%		10	5.13×10^6	2.02	%	5.29×10^6
2	He	0.00917	ppm			0.601	0.00917	ppm	0.601
3	Li	1.45	ppm	−1.4	10	54.8	1.50	ppm	57.1
4	Be	0.0219	ppm	4.3	7	0.638	0.0249	ppm	0.73
5	B	0.775	ppm		10	18.8	0.870	ppm	21.2
6	C	3.48	%		10	7.60×10^5	3.45	%	7.58×10^5
7	N	0.295	%		15	5.53×10^4	0.318	%	5.99×10^4
8	O	45.90	%		10	7.53×10^6	46.4	%	7.66×10^6
9	F	58.2	ppm		16	804	60.7	ppm	843
10	Ne	0.00018	ppm			0.0023	0.00018	ppm	0.0023
11	Na	4962	ppm	−0.6	9	5.67×10^4	5000	ppm	5.74×10^4
12	Mg	9.54	%	−0.4	4	1.03×10^6	9.89	%	1.074×10^6
13	Al	0.840	%	−1.2	6	8.17×10^4	0.868	%	8.49×10^4
14	Si	10.70	%		3	1.00×10^6	10.64	%	1.00×10^6
15	P	985	ppm	1.9	8	8.34×10^3	1220	ppm	1.04×10^4
16	S	5.35	%		5	4.38×10^5	6.25	%	5.15×10^5
17	Cl	698	ppm		15	5.17×10^3	704	ppm	5.24×10^3
18	Ar	0.00133	ppm			0.0096	0.00133	ppm	0.0096
19	K	546	ppm	0.4	9	3.67×10^3	558	ppm	3.77×10^3
20	Ca	0.911	%	−1.2	6	5.97×10^4	0.928	%	6.11×10^4
21	Sc	5.81	ppm	−1.5	6	33.9	5.82	ppm	34.2
22	Ti	447	ppm	−1.1	7	2.43×10^3	436	ppm	2.40×10^3
23	V	54.6	ppm	0.6	6	281	56.5	ppm	293
24	Cr	2623	ppm	−1.0	5	1.32×10^4	2660	ppm	1.35×10^4
25	Mn	1916	ppm	−0.7	6	9.15×10^3	1990	ppm	9.55×10^3
26	Fe	18.66	ppm	1.0	4	8.77×10^5	19.04	ppm	9.00×10^5
27	Co	513	ppm	1.4	4	2.28×10^3	502	ppm	2.25×10^3
28	Ni	1.091	%	0.9	7	4.83×10^4	1.10	%	4.93×10^4
29	Cu	133	ppm	1.5	14	549	126	ppm	522
30	Zn	309	ppm	−4.3	4	1.24×10^3	312	ppm	1.26×10^3
31	Ga	9.62	ppm	−0.9	6	36.2	10.0	ppm	37.8
32	Ge	32.6	ppm		9	118	32.7	ppm	119
33	As	1.74	ppm		9	6.10	1.86	ppm	6.56
34	Se	20.3	ppm		7	67.53	18.6	ppm	62.1
35	Br	3.26	ppm		15	10.7	3.57	ppm	11.8
36	Kr	5.22×10^{-5}	ppm			1.64×10^{-4}	5.22×10^{-5}	ppm	1.64×10^{-4}
37	Rb	2.32	ppm	0.4	8	7.13	2.30	ppm	7.09
38	Sr	7.79	ppm	−0.3	7	23.3	7.80	ppm	23.5
39	Y	1.46	ppm	−4.6	5	4.31	1.56	ppm	4.64
40	Zr	3.63	ppm	0.3	5	10.4	3.94	ppm	11.4
41	Nb	0.283	ppm	1.4	10	0.800	0.246	ppm	0.698
42	Mo	0.961	ppm	−1.2	10	2.66	0.928	ppm	2.55
44	Ru	0.690	ppm	0.6	5	1.79	0.712	ppm	1.86
45	Rh	0.132	ppm	−5.0	5	0.337	0.134	ppm	0.344
46	Pd	0.560	ppm	0.4	4	1.38	0.560	ppm	1.39
47	Ag	0.201	ppm		9	0.489	0.199	ppm	0.486
48	Cd	0.674	ppm		7	1.49	0.686	ppm	1.61
49	In	0.0778	ppm		5	0.168	0.080	ppm	0.184
50	Sn	1.63	ppm		15	3.35	1.720	ppm	3.82
51	Sb	0.145	ppm		14	0.300	0.142	ppm	0.309
52	Te	2.28	ppm		7	4.56	2.320	ppm	4.81
53	I	0.53	ppm		20	1.05	0.433	ppm	0.90
54	Xe	1.74×10^{-4}	ppm			3.48×10^{-4}	1.74×10^{-4}	ppm	3.48×10^{-4}
55	Cs	0.188	ppm	0.0	6	0.371	0.187	ppm	0.372
56	Ba	2.42	ppm	0.4	5	4.63	2.340	ppm	4.49
57	La	0.2414	ppm	−0.3	3	0.4561	0.2347	ppm	0.4460
58	Ce	0.6194	ppm	−0.4	3	1.160	0.6032	ppm	1.136
59	Pr	0.09390	ppm	−1.8	3	0.1749	0.0891	ppm	0.1669

(*Continued*)

Table 3 (Continued)

		Lodders et al. (2009), updated (1)					*Anders and Grevesse (1989) (2)*		
Element		*Mean CI abundance (by mass)*		*Δ in % relative to (1)*	*Estimated accuracy in (%)*	*Atoms per 10^6 atoms of Si*	*Mean CI abundance (by mass)*		*Atoms per 10^6 atoms of Si*
60	Nd	0.4737	ppm	0.6	3	0.8621	0.4524	ppm	0.8279
62	Sm	0.1536	ppm	1.0	3	0.2681	0.1471	ppm	0.2582
63	Eu	0.05883	ppm	1.8	3	0.1016	0.0560	ppm	0.0973
64	Gd	0.2069	ppm	0.9	3	0.3453	0.1966	ppm	0.3300
65	Tb	0.03797	ppm	−1.1	3	0.06271	0.0363	ppm	0.0603
66	Dy	0.2558	ppm	0.3	3	0.4132	0.2427	ppm	0.3942
67	Ho	0.05644	ppm	−1.3	3	0.08982	0.0556	ppm	0.0889
68	Er	0.1655	ppm	1.5	3	0.2597	0.1589	ppm	0.2508
69	Tm	0.02609	ppm	−0.02	3	0.04054	0.0242	ppm	0.0378
70	Yb	0.1687	ppm	−0.2	3	0.2559	0.1625	ppm	0.2479
71	Lu	0.02503	ppm	−1.0	3	0.03755	0.0243	ppm	0.0367
72	Hf	0.1065	ppm	0.5	3	0.1566	0.104	ppm	0.154
73	Ta	0.015	ppm	3.5	10	0.0218	0.0142	ppm	0.0207
74	W	0.096	ppm	0.0	10	0.137	0.0926	ppm	0.133
75	Re	0.0400	ppm	1.8	5	0.0554	0.0365	ppm	0.0517
76	Os	0.495	ppm	0.4	5	0.683	0.486	ppm	0.675
77	Ir	0.469	ppm		5	0.640	0.481	ppm	0.661
78	Pt	0.925	ppm	−2.3	5	1.24	0.990	ppm	1.34
79	Au	0.148	ppm	1.4	12	0.197	0.140	ppm	0.187
80	Hg	0.35	ppm		50	0.41	0.258	ppm	0.34
82	Tl	0.140	ppm	−1.4	11	0.184	0.142	ppm	0.184
82	Pb	2.62	ppm	−0.4	8	3.32	2.470	ppm	3.15
83	Bi	0.110	ppm		9	0.138	0.114	ppm	0.144
90	Th	0.0300	ppm	−3.2	7	0.0339	0.0294	ppm	0.0335
92	U	0.00810	ppm		7	0.00893	0.0081	ppm	0.0090

(1) Data from Lodders et al. (2009); (2) average CI abundances from Anders and Grevesse (1989), **Table 1**, columns 6 and 2, except C, N, O, and rare gases that are only from Orgueil. Δ relative to (1) – percent change of new values relative to Lodders et al. (2009).

abundances because of their low refractory element contents and their fractionated Mg/Si ratios (**Figure 3**).

The new photospheric lead determination (**Table 1**) now agrees with the CI chondritic lead abundance, within uncertainties. Thus, the excellent match of CI chondrites with the solar photosphere can be extended to some rather volatile elements (see **Section 2.2.1.5.1**).

Among chondrites, the CI chondrites have the highest contents of volatile elements including oxygen (a large fraction of it in the form of water). However, in contrast to other volatile elements, such as lead, the relative amount of oxygen contained in CI chondrites is still a factor of 2 below that of the solar photosphere (**Figure 3**), implying that oxygen was not fully condensed or water ice was never present on the meteorite parent body or lost. Furthermore, oxygen is expected to condense as water, but the conversion of the dominant high-temperature oxygen-bearing gas, CO, is also kinetically inhibited at low temperatures and may prevent CO conversion to water gas. If so, the formation of water ice does not occur above 180 K, but only at lower temperatures where water partial pressure matches the water ice vapor pressure (see Lodders, 2003). The concept of incomplete condensation of volatile elements in most meteorite groups is supported by the observation that there is no group of meteorites that is enriched in these elements relative to the average solar system abundances. There was no late redistribution of volatiles, for example, by reheating. In CI chondrites, the moderately volatile elements are fully condensed; other groups of chondrites acquired lower fractions of volatiles because of the solar gas dissipated during condensation (Palme et al., 1988; Wai and Wasson, 1977).

In summary, only one group of meteorites, the CI chondrites, closely matches the solar abundances for elements representing the various cosmochemical groups, except for the highly volatile elements, including the rare gases, hydrogen, carbon, oxygen, and nitrogen, and also the element lithium, which is destroyed by nuclear reactions in the Sun. All other chondrite groups deviate from solar abundances, and the deviations can be understood, at least in principle, by gas–solid fractionation processes before accretion of solid objects in the early solar system.

2.2.1.4.2 CI chondrites

Among the more than 40 000 recovered meteorites, there are only five CI chondrites: Orgueil, Ivuna, Alais, Tonk, and Revelstoke. These meteorites are very fragile and are easily fragmented on atmospheric entry. In addition, their survival time against weathering processes on Earth is short. All five CI meteorites are observed falls. Most analyses have been performed on the Orgueil meteorite, because it is the largest CI chondrite and material is easily available for analysis. However, problems with sample size, sample preparation, and the mobility of some elements are reflected in the chemical inhomogeneities within the Orgueil meteorite and often make it difficult to compare data by different authors. This contributes

significantly to the uncertainties in CI abundances (e.g., Morlok et al., 2006).

The chemical composition of CI chondrites as shown in Figure 3 demonstrates the reason for designating CI chondrites as primitive or unfractionated: there is good agreement with solar abundances. Texturally and mineralogically, they are far from being primitive. CI meteorites are microbreccias with millimeter to submillimeter clasts with variable composition. Late stage fractures filled with carbonates, hydrous calcium, and magnesium sulfate demonstrate that low-temperature processes have affected the meteorite (Morlok et al., 2006). The CI chondrites have essentially no chondrules and consist almost entirely of extremely fine-grained hydrous silicates with about 11% magnetite (Hyman and Rowe, 1983). High-temperature phases such as olivine and pyroxene are frequently found (Dodd, 1981; Lodders and Fegley, 2011). Although the CI chondrites undoubtedly match solar abundances very closely, their present texture and mineralogy have been largely established by processes that occurred late on the Orgueil parent body. On a centimeter scale, these processes must have been essentially isochemical; otherwise, the composition of Orgueil would not be solar for so many elements.

2.2.1.4.3 The CI chondrite abundance table

The abundance table (Table 3) is an update of an earlier compilation in Landolt–Börnstein by Lodders et al. (2009). It mainly uses data for the Orgueil meteorite as CI standard rock, because it is the most massive of the five CI chondrite falls and therefore the most analyzed one. Another approach was taken by Lodders (2003), who used data from all CI chondrites and computed weighted average compositions. Here, the authors also primarily rely on Orgueil data for CI abundances. A comparison of data for Orgueil with other CI chondrites can be found in Lodders (2003). As pointed out by Lodders et al. (2009), there are no systematic differences among CI chondrites, except that data from Ivuna, Alais, and Tonk seem to be more variable than those of Orgueil, which could also result from smaller sample sizes used for the less massive meteorites.

In this work, new analytical data for the Orgueil meteorite published after 2009 have been considered. As in Lodders et al. (2009), an estimated uncertainty was assigned for each element. In cases where the quality of individual analyses is roughly comparable, the uncertainty reflects the spread in individual Orgueil analyses. If only very few analyses were available, the uncertainties given by the authors were adopted. The distinction between accuracy and precision is not clear in all cases, as some authors prefer to give only estimates for precision. The listed uncertainties in Table 3 should roughly correspond to an estimate of the quality of the CI chondrite values. In cases where precision is high but accuracy low, larger uncertainties have been assigned than those given by the authors.

One problem is that in many cases, small Orgueil samples were used for bulk analysis, and the results may thus not be representative of the bulk Orgueil meteorite. The new data discussed in the succeeding text confirm the chemical homogeneity of Orgueil on a macroscopic or gram scale. But analyses of smaller samples often show fractionations in trace elements, despite high accuracy that was verified by analyses of standard rocks.

Barrat et al. (2012) published a comprehensive set of new analyses of 47 elements in CI chondrites. These authors measured six sample chips of Orgueil with masses between 0.62 and 1.020 g that were taken from five individual stones of Orgueil. In addition, they report data for Alais and Ivuna. The concentrations of some major and several trace elements were determined by inductively coupled plasma atomic emission spectrometry (ICP-AES). Most trace elements were, however, analyzed by inductively coupled plasma sector field mass spectrometry (ICP-SFMS). The variations in trace element contents in Orgueil samples are in general small, and s.d. of analyses of the various Orgueil samples are below 5% in most cases. Exceptions are the alkali elements sodium, potassium, rubidium, cesium, tungsten, and uranium (7–20% s.d.), and for tantalum, lead, and niobium (6–7% s.d.), marginally larger s.d. are reported.

The analyses of Barrat et al. (2012) include aliquots from six homogenized samples of 4.95 g in total, which represents a much larger fraction of Orgueil than used in most of published analyses. The basic agreement of these data with earlier data and the chemical homogeneity of Orgueil indicated by their new data demonstrate that the Orgueil meteorite is chemically homogeneous on a one-gram scale and thus has a well-defined chemical composition. The somewhat larger variability of alkali elements, tungsten, and uranium is not surprising in view of the mobility of these elements in fluids. Nevertheless, the difference between the highest and lowest Na concentration found in samples by Barrat et al. (2012) is only a factor of 2, and the average is within the range of many other analyses. On a micrometer scale, Orgueil is much more inhomogeneous; in particular, iron is decoupled from magnesium, silicon, aluminum, etc., elements that are primarily hosted in phyllosilicates (Morlok et al., 2006 and references therein), whereas larger fractions of iron are in magnetite.

The data by Barrat et al. (2012) also confirm that Alais and Ivuna have essentially the same composition as Orgueil. A study of REE, scandium, and yttrium in six representative Orgueil samples, two samples from Ivuna, and one from Alais reported by Pourmand et al. (2012) leads to the same conclusions.

Both data sets (Barrat et al., 2012; Pourmand et al., 2012) were used in revising the Lodders et al. (2009) data. The five representative Orgueil analyses were used recommended by Barrat et al. (2012). A comparison of the average of these samples with the CI chondrite abundances of Lodders et al. (2009) shows excellent agreement between both data sets. The largest difference between the two data sets is found for tungsten, at about 15%. The three elements aluminum, calcium, and thorium differ by more than 5%. All other elements agree within 5% (see Barrat et al., 2012).

In Table 3, the authors have listed their new compilation. In column 5, the difference in percent has been given relative to the Lodders et al. (2009) data resulting from addition of the new data to the authors' CI chondrite data collection. For some elements, ratios were used that are often more reliable, in particular when using data from other carbonaceous chondrites for comparison. In the following section, the major updates are briefly described.

For more than half of the elements, new average values were calculated. All changes are within 5%. The largest increases are for beryllium (4.3%) and tantalum (3.5%), the largest

decreases are for zinc (−4.3%), yttrium (−4.6%), rhodium (−5%), and thorium (−3.2%).

In the aqueous environment of Orgueil, *calcium* is much more variable than aluminum. The authors, therefore, calculated the calcium abundance from a carbonaceous chondrite average Ca/Al ratio of 1.085 (see Lodders et al., 2009), using the new aluminum abundance.

For *scandium*, the new data of Barrat et al. (2012) and Pourmand et al. (2012) led to a decrease of 1.5% (**Table 3**).

For *lead*, the new data from Baker et al. (2010) were considered in addition to the Barrat et al. (2012) data. The net result is a decrease in abundance by 0.4%.

New Orgueil data for *barium* and *cesium* by Hidaka and Yoneda (2011) were added to the data of Barrat et al. (2012). For barium, a change of 0.4% was calculated, and the new average for cesium is identical to the old value.

Special procedures were adopted for the following elements.

Yttrium. Pack et al. (2007) determined an Y/Ho ratio of 25.94 ± 0.08 for carbonaceous chondrites. With the authors' Ho concentration of 0.05644 ppm (see succeeding text), a Y concentration of 1.46 ppm is obtained. The CI chondrite Y concentration of Barrat et al. (2012) is 1.56 ppm and that of Pourmand et al. (2012) is 1.396 ppm, a discrepancy that almost certainly reflects analytical problems in one of the data sets, given the small variations in REE contents (see succeeding text). The two Orgueil analyses by Makishima and Nakamura (2006) are 1.49 and 1.43 ppm, slightly below 1.50 ppm. Their Y/Ho ratios (25.95 and 25.37) are within the chondritic value found by Pack et al. (2007). There are only a few older and less accurate data on yttrium in CI chondrites, so Y = 1.46 ppm is recommended from the Y/Ho ratio by Pack et al. (2007) (see Barrat et al., 2012, for an alternative view). Further careful analyses are required to resolve this question and provide a reliable CI chondritic Y concentration independently.

Zirconium, niobium, and tantalum. The average Orgueil Hf concentration used here is 0.1065 ppm (see succeeding text). With a Zr/Hf ratio of 34.12 (Lodders et al., 2009), the authors obtain a Zr concentration of 3.63 ppm, which is almost identical to the value of 3.62 ppm listed in Lodders et al. (2009). A Zr/Hf ratio of 34.1 ± 0.3 was reported for carbonaceous chondrites by Patzer et al. (2010). Their analyses are based on the same standard rocks as Münker et al. (2003) who obtained a chondritic Zr/Hf ratio of 34.3 ± 0.3, using isotope dilution with multicollector inductively coupled mass spectrometry. In Lodders et al. (2009), the CI chondritic niobium content was derived from the average Zr/Nb ratio of 12.93 in carbonaceous chondrites by Münker et al. (2003) and the Zr/Nb ratio of four Orgueil samples by Lu et al. (2007). Adding the Barrat et al. (2012) Zr/Nb ratio of 12.18 gives a mean Zr/Nb ratio of 12.55 that leads to a Nb concentration of 0.289 ppb, almost identical to the mean of 16 Orgueil analyses of 0.286 ppm. A similar procedure was applied to the Nb/Ta ratio. The mean chondritic Nb/Ta ratio of 20.4 by Münker et al. (2003) and 17.99 by Lu et al. (2007) and the new Barrat et al. (2012) ratio of 19.52 leads to a Ta concentration of 0.015 ppm.

The new average *REE* abundances have been calculated, using the mean of five samples from Barrat et al. (2012), five samples from Pourmand et al. (2012), and the Lodders et al. (2009) REE abundances. In **Figure 4**, the authors plot the average calculated REE abundances (new average: full red circles in **Figure 4**) as well as the individual data sets, all normalized to the REE data of Lodders et al. (2009). Deviations from their older data are given in percent. For comparison, isotope dilution data from Beer et al. (1984) and the Anders and Grevesse (1989) REE data have been added. These latter values deviate significantly from other data sets. Their abundances are not fully based on measurements for all REE but included some theoretical considerations (see Anders and Grevesse, 1989; and Lodders, 2003). The REE data from Lodders et al. (2009) were primarily taken from work using isotope dilution by thermal ionization mass spectrometry (TIMS) and by ICP-MS, with and without isotope dilution, and their new average Orgueil REE concentrations are essentially an average of REE determinations with mass spectrometric methods, with some more weight given to the new analyses.

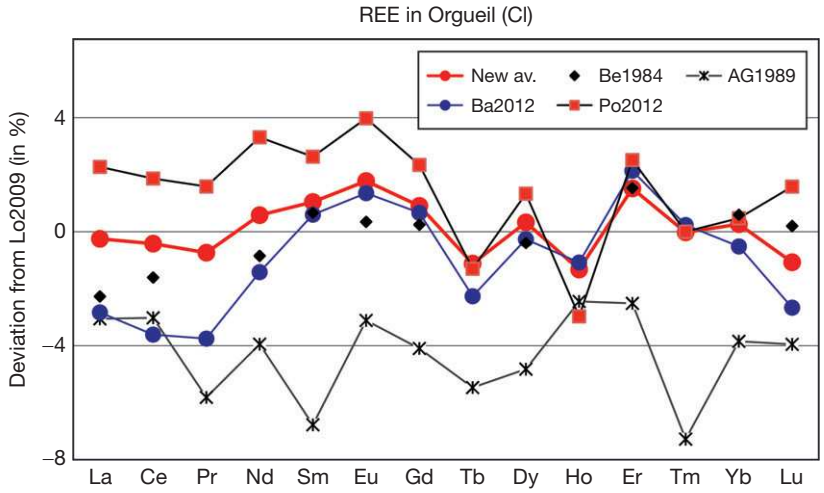

Figure 4 REE abundances in Orgueil. All data are normalized to the abundances listed in Lodders et al. (2009). The authors' new average is in most cases between the data of Barrat et al. (2012) and Pourmand et al. (2012), a consequence of the averaging procedure (see text). The Beer et al. (1984) data fit well with the new average. The Anders and Grevesse (1989) abundances are systematically lower (see text).

Variations in REE abundances from the two new studies of Barrat et al. (2012) and Pourmand et al. (2012) encompass the average concentrations from Lodders et al. (2009). Differences among individual data sets are fairly small, in all cases below 4% (**Figure 4**). This is only slightly above the relative s.d. given by Barrat et al. (2012) and Pourmand et al. (2012). The variations in Orgueil REE are larger for the LREE (light REE) than for HREE (heavy REE). This may be a result of the higher mobility of LREE in aqueous fluids. Compared to the authors' previous abundance recommendation, the largest changes for the new recommended REE abundances are for Pr (−1.8%), Eu (+1.8%), Ho (−1.3%), and Er (+1.5%). The Sm/Nd ratio of their new average Orgueil composition is 0.3242 in agreement with the Sm/Nd ratio of 0.3246 obtained by Bouvier et al. (2008) on Orgueil. This is consistent with the average Sm/Nd ratio of 14 carbonaceous chondrites of 0.3250 ± 0.0029, analyzed by Bouvier et al. (2008), whereas Barrat et al. (2012) have a higher mean Orgueil ratio of 0.3297 and Pourmand et al. (2012) a lower ratio of 0.3207 (see **Figure 4**).

For *hafnium*, the average of Lodders et al. (2009) and Barrat et al. (2012) is taken, as Pourmand et al. (2012) have not determined hafnium. This gives a Hf concentration of 0.1065 ppm, compared to 0.106 ppm listed by Lodders et al. (2009). With this value and the new Lu concentration (**Table 3**), a Lu/Hf ratio of 0.2347 is obtained. This is less than a percent below the ratio from Lu–Hf dating of 0.2368 by Bouvier et al. (2008).

The Hf/W ratios are used to determine the *tungsten* content of CI chondrites. Several recent analyses are available for carbonaceous chondrites because the Hf/W ratio is important for radiometric Hf–W dating. Both Hf and W are refractory elements, and their concentration ratio appears be relatively constant within the various types of carbonaceous chondrites. The average Hf/W ratio of 2 Orgueil samples, 5 Allende splits, and 12 other carbonaceous chondrites analyzed by Kleine et al. (2004) is 1.11 ± 0.13 ppm. A Hf concentration of 0.1065 ppm leads to a W concentration of 96 ± 10 ppb, in agreement with the earlier data by Rammensee and Palme (1982). The W abundance of 110 ppb by Barrat et al. (2012) is nearly 15% above the authors' estimate. This is the largest discrepancy between the Barrat et al. (2012) abundance table and the compilation presented here. The CI chondritic Hf concentration is well established with 0.1065 ppm. The critical issue is, however, the CI chondritic Hf/W ratio. Two Orgueil samples analyzed by Kleine et al. (2004) gave a Hf/W ratio about unity (1.035 and 0.974), significantly lower than the Hf/W ratio of 1.112 in the CV chondrite Allende by the same authors. This agrees with the Hf/W ratio of three Allende samples of 1.141 by Yin et al. (2002) but disagrees with the Barrat et al. (2012) ratio of 1.01, which is very close to the Orgueil Hf/W ratio (0.973) by the same authors. An Orgueil Hf/W ratio of 1.12 is reported in a recent paper by Babechuk et al. (2010), although both concentrations Hf and W are untypically low for Orgueil. Two questions need to be clarified (a) is the Hf/W ratio variable in different types of carbonaceous chondrites and (b) is tungsten much more mobile in CI chondrites than hafnium? There is thus a need for precise and representative tungsten analyses in the Orgueil meteorite and in other carbonaceous chondrites, with simultaneous analyses of other elements that allow to judge if the analyzed sample is representative of Orgueil.

Ruthenium, rhodium, palladium, rhenium, osmium, iridium, platinum, and gold. Fischer-Gödde et al. (2010) have recently analyzed abundances of highly siderophile elements (HSE) in chondritic meteorites. The HSE comprise six platinum group elements (PGE) – ruthenium, rhodium, palladium, osmium, iridium, and platinum – rhenium and gold. Except for palladium and gold, these elements are refractory noble metals condensing at temperatures above FeNi alloys, whereas palladium and gold have condensation temperatures below FeNi. The authors included the new analyses for palladium and gold in Orgueil to their list and calculated new averages, which are within 0.4% (Pd) and 1.4% (Au) of the old values, listed in Lodders et al. (2009). The abundance level of the refractory metals in the analyses of Fischer-Gödde et al. (2010) is however about 10% below that of most Orgueil analyses. The literature average of more than 40 iridium analyses of Orgueil is 469 ppb, compared to the results of Fischer-Gödde et al. (2010) with 421 ppb. A similarly low value was found by Horan et al. (2003). Other refractory metals vary similarly. The reason for the low abundances of the refractory metals is unclear. There are excellent correlations among refractory metals, which are identical in the data sets by Horan et al. (2003) and Fischer-Gödde et al. (2010). These authors have therefore scaled their abundances of refractory metals to the Ir concentration in Orgueil, which they determined to be 462 ppb from a large number of literature analyses, slightly below the average of 469 ppb estimated by Lodders et al. (2009). Because of the constancy of the refractory metal ratios in carbonaceous chondrites and the excellent agreement between the data of Horan et al. (2003) and Fischer-Gödde et al. (2010), the authors have used these ratios to calculate the abundances of the other refractory metals based on an Ir concentration of 0.469 ppm. This leads to slightly different abundances than those listed in Lodders et al. (2009). The largest change is for rhodium that is now 5% below the old value. The element ratios used and the resulting Orgueil abundances are given in **Table 4**.

A comparison with the Anders and Grevesse (1989) compilation (**Table 3**) shows that there are no dramatic changes in the analytical Orgueil abundances since the last 20 years, except for the REE elements (see discussion in the preceding text). Differences above 10% between the new data in **Table 3** and the Anders and Grevesse (1989) compilation are found in only a few cases: boron (12%), niobium (13%), beryllium (14%), sulfur (17%), iodine (18%), phosphorus (24%), and mercury (26%). There are 16 elements with differences between 5% and 10%. All other elements agree to within 5%. Presently, analytical tools allow precise and accurate chemical analyses of most elements.

The data of Barrat et al. (2012), who probably analyzed the largest fraction of Orgueil, are in excellent agreement with the authors' data compiled from various sources. The largest differences are for tungsten and yttrium. As discussed before, a W concentration of Orgueil of 0.096 ppm has been obtained compared to 0.11 ppm by Barrat et al. (2012). For the Y concentration, the authors use 1.46 ppm compared to 1.56 ppm by Barrat et al. (2012). In both cases, the authors have used element ratios Hf/W and Y/Ho for establishing their preferred CI concentration, as constant element ratios may be occasionally used to better define CI chondrite composition. This method assumes,

Table 4 Concentration ratios and concentration of refractory metals in carbonaceous chondrites

Concentration ratios of refractory metals in CI chondrites						
	Os/Re	Os/Ir	Os/Ru	Pt/Ir	Pt/Rh	
Horan et al. (2003)	12.270	1.056	0.7231	1.904		
Fischer-Gödde et al. (2010)	12.493	1.053	0.7117	2.043	7.26	
Average ratio	12.381	1.055	0.7174	1.974	7.26	
Concentrations of refractory metals in CI chondrites, in ppm						
	Ru	Rh	Re	Os	Ir	Pt
Fischer-Gödde et al. (2010)[a]	0.688	0.133	0.0407	0.491	0.462	0.943
Lodders et al. (2009)	0.686	0.139	0.0393	0.493	0.469	0.947
This work[b]	0.690	0.132	0.0400	0.495	0.469	0.925

[a]Based on CI concentration of Ir of 0.462 ppm.
[b]Based CI Ir concentration of 0.469 ppm and using average refractory element ratios.

however, constant refractory element ratios in chondritic meteorites. During the last years, it has been demonstrated that refractory elements are slightly fractionated in various groups of chondritic meteorites. For example, Os/Re and the Y/Ho ratios show small variations in different groups of chondritic meteorites (Pack et al., 2007; Walker et al., 2002).

Further progress will not come from improvements of analytical techniques. It will be more important to define and analyze a representative sample of CI and other chondrites and determine major, minor, and trace elements on exactly the same aliquots. Sample homogeneity and analysis of the 'right' sample will be the limiting factors for improving the meteoritic data basis.

2.2.1.5 Solar System Abundances of the Elements

2.2.1.5.1 Comparison of meteorite and solar abundances

In Table 1, the silicon-normalized meteorite abundances of Table 3 ($\log A_{Si} = 6$) are converted to the hydrogen-normalized abundances ($\log A_H = 12$). The conversion factor between the two scales was calculated by dividing the hydrogen-normalized solar abundances by the silicon-normalized meteorite abundances. The comparison was made for all elements with an error of the corresponding photospheric abundance of less than 0.1 dex, that is, less than about 25%. Manganese and hafnium were excluded because the discrepancies between meteoritic and solar abundances are much larger than expected from the uncertainties (see succeeding text). Thirty-eight elements qualified for this procedure, and the log of the average ratio of *solar abundance per 10^{12} H atoms/meteorite abundance per 10^6 Si atoms* is 1.5332 ± 0.030. Thus,

$$\log A_{ast} = \log A_{met} + 1.533$$

This yields a silicon abundance on the astronomical scale of $\log A_{ast}(Si) = 7.533$ and a hydrogen abundance on the meteoritic scale of $\log A_{met}(H) = 10.47$ or 2.95×10^{10} atoms relative to 10^6 Si atoms. Within uncertainties, the conversion factor determined here is close to that of earlier determinations. Anders and Grevesse (1989) calculated a value of 1.554, while Lodders (2003) used 1.540. In the first edition Palme and Jones found 1.546 and Lodders et al. (2009) 1.533 ± 0.042, identical to the present value, but slightly less precise.

In column 6 of Table 1, all meteorite data are given on the astronomical scale. The calculation was done by adding 1.533 to the data based on 10^6 Si atoms. These ratios are displayed in Figure 5. The solar abundances of carbon, nitrogen, and oxygen are higher because these elements are incompletely condensed in CI chondrites.

In Figure 6, the Sun/CI chondrite abundance ratios (in atoms) of 45 elements are plotted versus their atomic number. All elements plotted have uncertainties in their photospheric abundance of $\leq$0.1 dex (about 25%). There are 36 elements with Sun/Orgueil abundance ratios between 0.9 and 1.1. Among these are lithophile, siderophile, and chalcophile elements. The elements lanthanum, ytterbium, ruthenium, copper, lead, and terbium lie within the $\pm$20% limit. Problematic elements are tungsten, rubidium, gallium, hafnium, and manganese, as the differences in abundance between the Sun and CI chondrites are larger than the error bars of the Sun/CI chondrite ratios (see Lodders et al., 2009). The uncertainties assigned to the solar abundance determinations of tungsten, rubidium, and gallium are 40%, 25%, and 25%, much less than the abundance differences, which are factors of 2.75, 1.63, and 0.61, respectively (Table 1). The estimated uncertainty of the Orgueil concentrations of these three elements is below 10%. The authors suspect either that the uncertainties of the photospheric determinations are underestimated or that there are unknown systematic errors involved. The abundances of tungsten, rubidium, and gallium need to be redetermined in the photosphere. The case is more serious for hafnium and manganese. The abundance differences are 35 and 30%, but the assigned errors of the solar/meteoritic ratios are 12 and 14% for hafnium and manganese, respectively. Manganese was recently redetermined in the Sun (Blackwell-Whitehead et al., 2011). The new solar abundance value is 10% below the old value increasing the discrepancy between solar and meteoritic abundance. Manganese can be accurately measured in meteorites. Its concentration in Orgueil is similar to that in two other CI meteorites, Alais and Ivuna, and it fits with the abundances of other elements of similar volatility. The Mn/Na ratio is, for example, constant in most carbonaceous chondrites (e.g., see Chapter 3.1), despite decreasing abundances of both elements with increasing petrologic type (from CI to CV) and despite very different geochemical behavior of manganese and sodium. The authors suspect that an unidentified problem

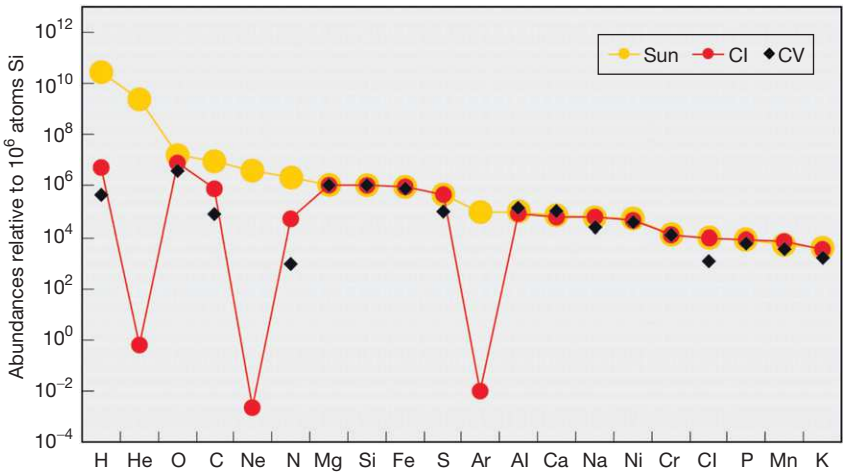

Figure 5 The abundances of the 20 most abundant elements in the Sun are compared with CI chondrite abundances. Rare gases show the largest depletion in Orgueil, followed by hydrogen, nitrogen, carbon, and oxygen. CV chondrites are also plotted. Their fit with solar abundances is worse than the fit with CI chondrites. A more detailed comparison between meteoritic and solar abundances is given in **Figure 6**.

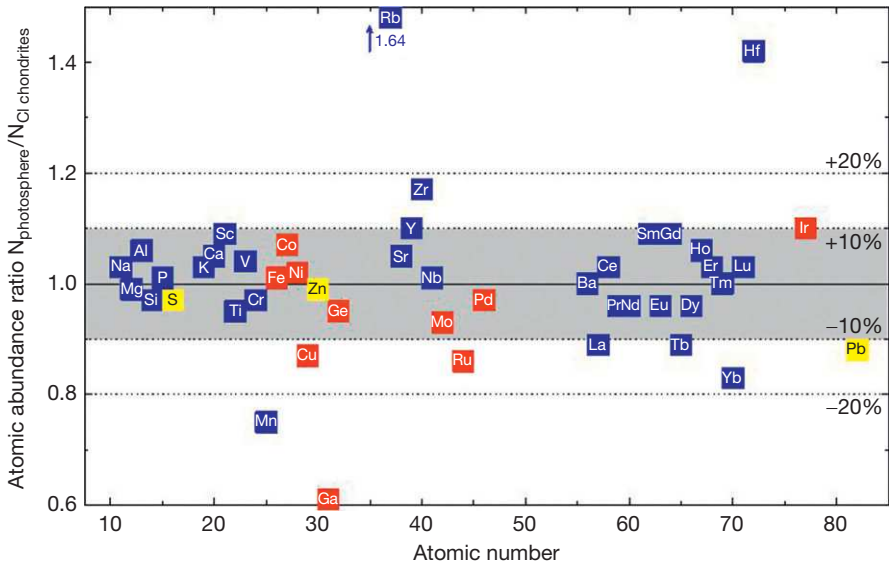

Figure 6 Comparison of photospheric and meteoritic (CI chondrite) abundances. Only elements with uncertainties below 0.1 dex (~25%) in the photospheric abundance determination are shown (data from **Table 1**). There are now 36 elements where meteoritic and photospheric abundances agree to within ±10%. Lithophile elements are blue, siderophile red, and chalcophile yellow. See text for details.

in the photospheric abundance analysis may cause the discrepancy of the meteoritic and solar manganese abundances.

The problem for manganese is reversed for hafnium: the meteoritic abundance of hafnium is less than that of the photosphere. This could indicate a problem with the photospheric abundance determination and suggest that line blending is more severe than already corrected for in current models. However, two recent hafnium analyses using different models essentially obtain the same abundance, and if there is a problem with the analysis, it remains elusive. The Hf concentration in CI chondrites has been accurately determined, because hafnium is important for Lu–Hf and W–Hf dating. The very constant Lu/Hf ratio discussed earlier closely ties hafnium to other refractory elements that do not show such large differences in abundance to the Sun as does hafnium. This issue awaits resolution.

In summary, the agreement between photospheric and meteoritic abundances is further improved with the new solar and meteoritic data. As shown in **Figure 6**, there is no apparent trend of solar/CI chondritic abundance ratios with increasing atomic number or increasing volatility (decreasing condensation

temperature) or any other property of the nuclides (see Lodders et al., 2009). In particular, the solar/CI chondritic abundance ratios are independent of the geochemical character of an element, whether it is lithophile, siderophile, and chalcophile.

The agreement between CI chondritic and solar abundances must be considered excellent, and there is not much room left for further improvements. Obvious candidates for redetermination in the solar photosphere are manganese, hafnium, rubidium, and tungsten.

2.2.1.5.2 Solar system abundances versus mass number

The isotopic compositions of the elements are not discussed in this contribution. The compilation by Lodders et al. (2009) contains a list of isotopes and their relative abundances. From these data, the abundances for individual mass numbers can be calculated using the elemental abundances of the elements as given in **Table 1**. **Figure 7** is a plot of abundances versus mass number. The generally higher abundances of even masses are apparent. Even and odd mass numbers plot along more or less smooth curves, with odd mass numbers forming a considerably smoother curve than even mass numbers. Historically, empirical abundance rules, established by Suess (1947), postulate a smooth dependence of isotopic abundances on mass number A, especially of odd-A nuclei. This was an important tool to estimate unknown or badly determined abundances. Later, this rule was modified and supplemented by two additional rules (Suess and Zeh, 1973) in order to make the concept applicable to the now more accurate abundance data. However, the smoothness of odd-A nuclei abundances itself has been questioned (Anders and Grevesse, 1989; Burnett and Woolum, 1990). The high abundance of ^{89}Y (**Figure 7**), an apparent discontinuity (Burnett and Woolum, 1990), reflects the low neutron capture cross section of a dominantly *s*-process nucleus with a magic neutron number (50). There is no smoothness of even-A (^{118}Sn and ^{138}Ba) or odd-A nuclei (^{89}Y) with mass number. Element abundances cannot be determined on the basis of smooth abundance curves.

2.2.1.5.3 Other sources for solar system abundances

The emission spectroscopy of the solar corona, the solar energetic particles (SEP), and the composition of the solar wind yield information on the composition of the Sun. Solar wind data were used for isotopic decomposition of rare gases. Coronal abundances are fractionated relative to photospheric abundances. Elements with high first ionization potential (FIP) are depleted relative to the one with low FIP (e.g., Anders and Grevesse, 1989).

Solar wind was collected by the Genesis spacecraft and returned to Earth, and the concentrations of increasing numbers of elements from the Genesis collectors are being reported. Additional data will allow a deeper understanding of elemental fractionation caused by acceleration of solar wind, and the Genesis data may one day become another reliable measure of photospheric composition. In a first step new isotopic data for oxygen and nitrogen from Genesis samples were published (McKeegan et al., 2011; Marty et al., 2011). These data should be considered when using the Lodders et al. (2009) data for the isotopic composition of elements.

The composition of dust grains of comet Halley has been determined with impact ionization time-of-flight mass spectrometers on board the Vega-I, Vega-II, and Giotto spacecraft. The abundances of 16 elements and magnesium, which are used for normalization, are on average CI chondritic to within factors of 2–3, except for hydrogen, carbon, and nitrogen, which are significantly higher in Halley dust, presumably due to the presence of organic compounds (Jessberger et al., 1988; Schulze et al., 1997). There is no evidence for a clear enhancement of volatile elements relative to CI chondrites.

Many of the micrometer-sized interplanetary dust particles (IDPs) have approximately chondritic bulk composition (see

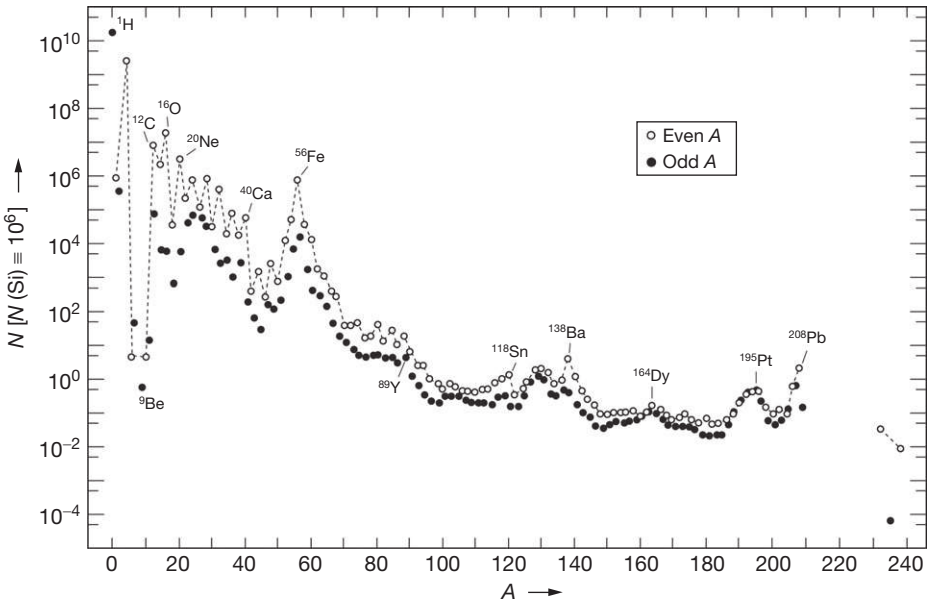

Figure 7 Solar system abundances by mass number. Atoms with even masses are more abundant than those with odd masses (Oddo–Harkins rule). There is no smooth dependence of abundances on mass numbers for even (e.g., ^{118}Sn and ^{138}Ba) or for odd masses (e.g., ^{89}Y).

Chapter 1.8 for details). Porous IDPs match the CI chondrite composition better than nonporous (smooth) IDPs. On average, IDPs show some enhancement of moderately volatile and volatile elements (see Palme, 2000). Arndt et al. (1996) found similar enrichments in their suite of 44 chondritic particles (average size 17.2 ± 1.2 μm). The elements chlorine, copper, zinc, gallium, selenium, and rubidium were enriched by factors of 2.2–2.7. These authors also reported very high enrichments of bromine ($29 \times$ CI) and arsenic ($7.4 \times$ CI), perhaps acquired in the Earth's atmosphere.

These particles probably come from the asteroid belt (Flynn et al., 1996). They are brought to Earth by the action of the Poynting–Robertson effect. They could be derived from objects that contain uncondensed volatiles from the inner part of the nebula, which would make comets an attractive source. These particles seem to be the only examples of a clear enhancement of moderately volatile elements over solar values in solar system material. Their proposed asteroidal origin would be at odds with a cometary origin, however, these samples could also come from extinct comets that are now part of the asteroid population (see Lodders and Osborne, 1999).

2.2.2 The Abundances of the Elements in the ISM

2.2.2.1 Introduction

The solar system was formed as the result of the collapse of a cloud of preexisting interstellar gas and dust (see Figure 8). A close compositional relationship should therefore be expected between the solar system and the interstellar material from which it formed. If the assumption is made that the composition of the ISM has remained unchanged since the formation of the solar system, the local ISM can be used as a measure of the original presolar composition. Differences between the solar system and current local ISM would imply that fractionation occurred during the formation of the solar system, that the local ISM composition changed after solar system formation, or that the solar system formed in a different part of the galaxy and then migrated to its present location. Studies of solar system and local ISM composition are therefore fundamental to the formation of the solar system, the nature of the local ISM, and the general processes leading to low-mass star formation.

The discovery and analysis of presolar grains in meteorites have enabled the precise chemical and isotopic analysis of interstellar material (e.g., Anders and Zinner, 1993; Chapter 1.4). The huge variations in the isotopic compositions of all elements analyzed in presolar grains are in stark contrast to the basically uniform isotopic composition of solar system materials. This uniformity would have required an effective isotopic homogenization of all the material in the solar nebula, that is, gas and dust, during the early stages of the formation of the solar system.

2.2.2.2 The Nature of the ISM

The ISM is the medium between the stars. For present purposes, the media immediately surrounding the stars (generally

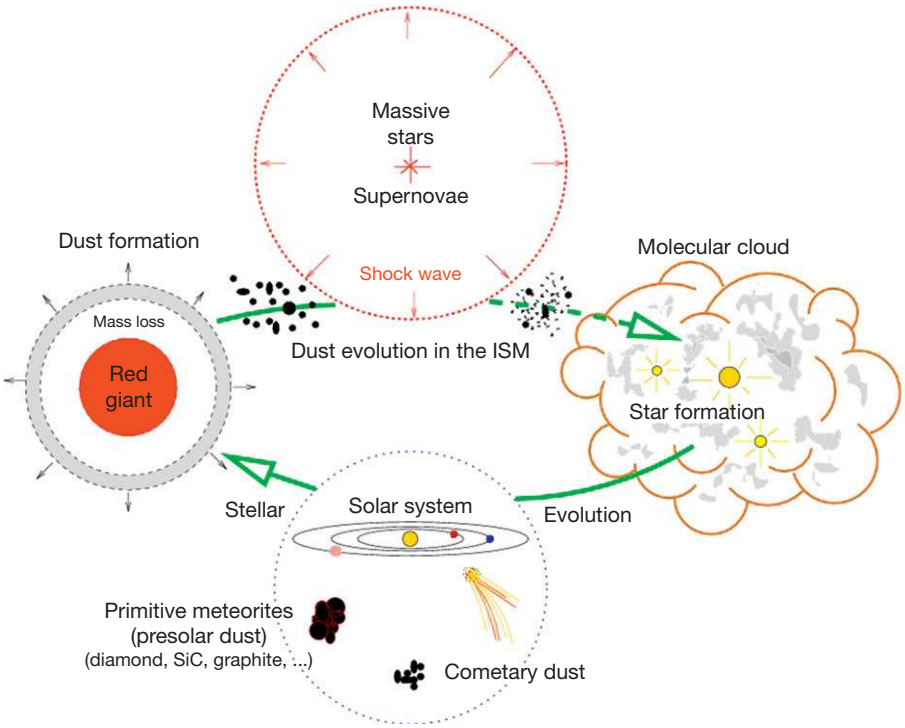

Figure 8 A schematic view of the life cycle of interstellar dust from its formation principally around evolved stars, and also to some extent in supernovae, to its incorporation into star-forming molecular clouds and planetary systems. Along the way, its properties evolve through energetic collisions with the gas and other grains in interstellar shock waves and through the effects of UV irradiation. Figure taken from Jones AP (2004) Dust destruction processes. In: Witt AN, Clayton GC, and Draine BT (eds.) *Astrophysics of Dust*. *ASP Conference Series*, Vol. 309, pp. 347–367. With permission from the Astronomical Society of the Pacific.

considered as circumstellar media) will also be considered as part of the ISM. Most of the matter in the ISM is in the form of a very tenuous gas with densities of less than one hydrogen atom per cubic centimeter to perhaps a million hydrogen atoms per cubic centimeter. For comparison, the terrestrial atmosphere contains about 10^{19} hydrogen atoms per cm^3.

Interstellar matter is comprised of both gas and dust. The gas consists of atomic and polyatomic ions and radicals and also of molecules. It is the form of hydrogen in the ISM that is used to describe its nature, that is, ionized (H^+), atomic (H), or molecular (H_2), with increasing density from ionized to molecular gas. The dust is primarily composed of amorphous carbon and silicates and makes up about 1% of the mass of the ISM. The dust particles have sizes in the nanometer to micrometer range (e.g., Mathis, 1990). The total amount of absorption and scattering along any given line of sight is called the interstellar extinction. The degree of extinction depends upon the wavelength, the size of the dust grains, and their composition.

2.2.2.3 The Chemical Composition of the ISM

2.2.2.3.1 The composition of the interstellar gas and elemental depletions

The elements incorporated into grains in the ISM cannot be observed directly. They are underrepresented in or depleted from the gas phase. Only the fraction of an element that remains in the gas phase can be detected in the ISM, provided that the element has accessible and observable transitions. Initial measurements of the abundances of elements in the gas phase date back to the mid-1960s, when with the advent of space missions, it became possible to observe above the absorbing effects of the Earth's atmosphere (e.g., Morton and Spitzer, 1966). With the sensitive spectrographs onboard the International Ultraviolet Explorer (IUE) and the Hubble Space Telescope (HST, e.g., the Goddard High Resolution Spectrometer, GHRS, and the Space Telescope Imaging Spectrograph, STIS), many lines of sight have now been studied for a large number of elements (e.g., Cartledge et al., 2001; Howk et al., 1999; Jenkins, 2009; Savage and Sembach, 1996).

Hydrogen and helium are the most abundant elements in the ISM gas phase. To date, more than 30 elements heavier than helium have been observed and their gas-phase abundances determined. Based on the existing data (e.g., Howk et al., 1999; Savage and Sembach, 1996; Sofia and Meyer, 2001), the local ISM sampled out to a few kiloparsecs from the Sun appears to be rather uniform in chemical composition. Recently, Jenkins (2009) has undertaken a detailed study of the differential depletion behaviors of 17 different elements, along lines of sight with $N(H) > 10^{19.5}$ cm^{-2}, and uncovered an interesting problem with the high depletion of oxygen (see **Section 2.2.2.3.3**).

Using a new approach, Sofia et al. (2011) measured the carbon gas-phase abundances along six lines of sight by profile-fitting strong ionized carbon (C^+ or CII) transitions in spectra continuum-normalized with stellar models. They compared their new abundance determinations to previous measurements for the same lines of sight that were made using weak CII lines to measure the carbon abundance. With this new approach, they conclude "that more carbon could reside in dust than was previously thought." It thus appears that, compared to earlier estimates, about 50% more dust-phase carbon is available to satisfy the observed interstellar extinction requirements.

As an example of the interstellar depletions, the authors show the results of abundance determinations along the line of sight toward ζ Oph (zeta Ophiuchus), a moderately reddened star that is frequently used as standard for depletion studies. Molecules are observed along this line of sight, and the material is a blend of cool diffuse clouds and a large cold cloud. The atomic hydrogen column density is $\log N(H) = 21.12 \pm 0.10$. In **Table 5**, all data are normalized to 10^{12} atoms of hydrogen, and in the last column, the ratios of the ζ Oph abundances to the solar abundances are given. In **Figure 9**, these ratios are plotted against condensation temperatures (see Savage and Sembach, 1996, for details). The abundances of many of the highly volatile and moderately volatile elements up to condensation temperatures of around 900 K (at 10^{-4} bar) are, within a factor of 2, the same in the ISM and in the Sun, independent of the condensation temperatures. This suggests that these elements predominantly reside in the gas phase in the ISM and that their elemental abundances in the ISM are similar to those of the solar system. At higher condensation temperatures, a clear trend of increasing depletions with increasing condensation temperatures is seen. The more refractory elements are condensed into grains in the outflows of evolved stars or perhaps in the dust in the ejected remnants associated with supernovae explosions.

There are several elements whose abundances deviate from the general trend (e.g., phosphorus and arsenic in **Figure 9**). It will be important to find out during the course of future work whether these deviations reflect problems with the extremely complex analyses or whether they are true variations that indicate particular chemical processes in the ISM or that could be characteristic of condensation in stellar outflows.

It should be emphasized that the depletion pattern in the ISM does not reflect thermodynamic equilibrium between dust and gas. The temperature in the ISM is so low that virtually all elements, including the rare gases, should be condensed in grains if thermodynamic equilibrium between dust and gas is maintained. The depletion pattern rather reflects conditions at higher temperatures established during the condensation of minerals in the outflows of dying stars or supernovae explosions. This pattern is then frozen in the cold ISM.

2.2.2.3.2 The composition of interstellar dust

As concluded in the previous section, the dust in the ISM is primarily composed of the elements carbon, oxygen, magnesium, silicon, and iron. This argument is based on the elemental makeup of the solid phase in the ISM determined from the depletions. However, the exact chemical and mineralogical composition of the dust in the ISM can only be determined through infrared observations of the absorption of starlight by cold dust ($T < 20$ K) along lines of sight toward distant stars and also by the emission features from hot dust ($T <$ a few hundred Kelvin) in the regions close to the stars. Such observations reveal the spectral signatures of amorphous aliphatic and aromatic hydrocarbons and amorphous silicates. In dense clouds (densities of the order of 10^3–10^5 H atoms cm^{-3}), where the matter is well shielded from the destructive effects

Table 5 Abundances of elements in the gas phase of the ISM in the direction of ζ Ophiuchus

Element T_c		*Solar system*		*ζ Ophiuchus cool*			*ζ Ophiuchus cool/solar*
	K	*log* X	*s.d.%*	*log* X	*s.d. %*	*Lit*	
Highly volatile elements							
C	40	8.59	30	8.14	35	Savage and Sembach (1996)	0.36
Ar	47	6.56	5	6.08	45	Savage and Sembach (1996)	0.33
Kr	52		15	2.97	15	Savage and Sembach (1996)	0.47
N	123	7.93	30	7.90	15	Savage and Sembach (1996)	0.93
O	180	8.47	20	8.48	15	Savage and Sembach (1996)	0.55
Moderately volatile elements							
Tl	532	0.81	60	1.27	30	Savage and Sembach (1996)	2.9
Cd	652	1.77	30	1.67	10	Sofia et al. (1999)	0.79
S	664	7.19	30	7.45	90	Savage and Sembach (1996)	1.8
Se	697	3.40		3.45	70	Savage and Sembach (1996)	1.1
Sn	704	2.12	90	2.16	25	Savage and Sembach (1996)	1.1
Te	709	2.22		<3.01		Savage and Sembach (1996)	<6.2
Zn	726	4.66	20	3.98	30	Savage and Sembach (1996)	0.21
Pb	727	2.05	15	1.34	40	Savage and Sembach (1996)	0.19
F	734	4.67	90	4.26	60	Snow et al. (2007)	0.25
Ge	883	3.62	40	3.01	10	Savage and Sembach (1996)	0.25
B	908	2.87	90	1.95	25	Savage and Sembach (1996)	0.12
Cl	948	5.26	90	5.27	60	Savage and Sembach (1996)	1.0
Na	958	6.30	5	5.36	25	Savage and Sembach (1996)	0.11
Ga	968	3.11	25	1.99	15	Savage and Sembach (1996)	0.076
K	1006	5.11	35	4.04	80	Savage and Sembach (1996)	0.085
Cu	1037	4.28	10	2.92	5	Savage and Sembach (1996)	0.044
As	1065	2.35	??	2.16	25	Savage and Sembach (1996)	0.65
Li	1142	3.30	10	1.73	15	Savage and Sembach (1996)	0.027
Mn	1158	5.51	5	4.08	5	Savage and Sembach (1996)	0.037
P	1229	5.44	10	5.07	75	Savage and Sembach (1996)	0.43
Mg silicates and metallic FeNi							
Cr	1296	5.67	5	3.4	5	Savage and Sembach (1996)	5.3×10^{-3}
Si	1310	7.55	15	6.24	5	Savage and Sembach (1996)	4.9×10^{-2}
Fe	1334	7.48	20	5.24	5	Savage and Sembach (1996)	5.7×10^{-3}
Mg	1336	7.56	15	6.33	5	Savage and Sembach (1996)	5.9×10^{-2}
Co	1352	4.90	10	2.15	30	Savage and Sembach (1996)	1.8×10^{-3}
Ni	1353	6.23	10	3.51	5	Savage and Sembach (1996)	1.9×10^{-3}
Refractory elements							
V	1429	3.99	5	<2.06		Savage and Sembach (1996)	$<1.2\times10^{-2}$
Ca	1517	6.33	5	2.61	15	Savage and Sembach (1996)	1.9×10^{-4}
Ti	1582	4.95	14	1.91	10	Savage and Sembach (1996)	9.2×10^{-4}

T_c – condensation temperatures at 10^{-4} bar (Lodders, 2003); log X – log of abundances relative to 10^{12} atoms of H; standard deviations are given to the nearest 5%.

of stellar UV light, the authors observe molecular species such as H_2, H_2O, CO, CO_2, and CH.

The interstellar carbon grains contain both aliphatic and aromatic C–H and C–C bonds; both are observed in absorption and emission in the ISM, but beyond this, their exact composition is not known. Given the seemingly uniform elemental abundances in the local ISM, the authors might expect that the dust composition would also be chemically uniform. However, the inferred elemental composition of silicates in the ISM indicates that they have an olivine-type stoichiometry where the depletions are largest, and a mixed oxide/silicate stoichiometry where lower depletions indicate that some dust erosion has occurred (e.g., Jones, 2000; Savage and Sembach, 1996, and references therein). In the lower density regions above the galactic plane, a different dust stoichiometry is clearly seen (e.g., Savage and Sembach, 1996). This change in composition is presumably a reflection of the effects of shock waves that have lifted interstellar clouds high above the plane and that have, at the same time, eroded and destroyed some fraction of the dust incorporated into these clouds.

2.2.2.3.3 Interstellar oxygen problems

Snow and Witt (1996) and others argued that the composition of the ISM is different from the composition of the Sun. Based on stellar compositional data, these authors concluded that heavy elements in the Sun are only two-thirds of the solar composition, with the implication that the heavy elements either fractionated from hydrogen during formation of the Sun (Snow, 2000) or that the Sun was formed in a different place in the Milky Way where the heavy element abundances

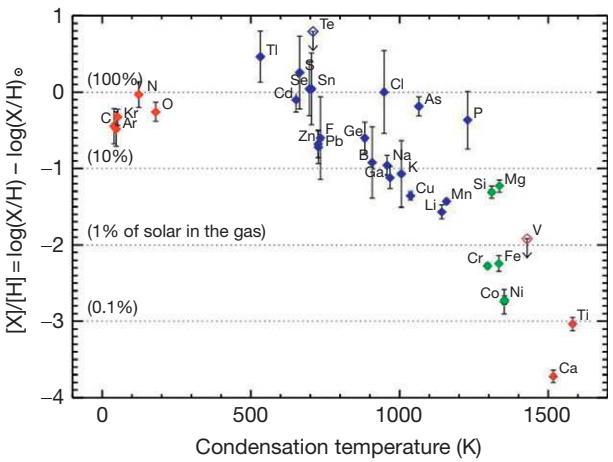

Figure 9 Abundances of the elements along the line of sight toward ζ Oph (ζ Ophiuchus), a moderately reddened star that is frequently used as standard for depletion studies. The ratios of ζ Oph abundances to the solar abundances are plotted against condensation temperatures. Reproduced from Savage BD and Sembach KR (1996) Interstellar abundances from absorption-line observations with the Hubble Space Telescope. *Annual Review of Astronomy and Astrophysics* 34: 279–329. With permission from Annual Reviews. The abundances of many of the highly volatile and moderately volatile elements (red and blue data points, respectively) up to condensation temperatures of around 700 K are, within a factor of 2, the same in the ISM and in the Sun. At higher condensation temperatures, a clear trend of increasing depletions with increasing condensation temperatures is seen for the silicate-forming and refractory elements (green and brown data points, respectively). It is usually assumed that the missing refractory elements are in grains. Upper limit values are indicated with open symbols and a downward arrow.

were higher. Another possibility was that there were additional 'hidden' reservoirs. In particular, there was a problem of too much interstellar oxygen when using the solar oxygen abundance as standard. Where could that excess oxygen be stored? Some 20% of the solar oxygen abundance must have been combined with magnesium, silicon, iron, etc., into the amorphous silicates observed in the ISM. Another 40% is directly observed in the gas as atomic oxygen (Meyer et al., 1998). The 'missing' 40% of oxygen remained elusive; it could not be in the form of molecules, for example, H_2O and CO, because they were not observed in sufficient abundance. The recent reevaluation of the solar oxygen abundance (Allende Prieto et al., 2001; Holweger, 2001) and of interstellar oxygen (Sofia and Meyer, 2001) has resolved this problem. The new solar oxygen is now only 60% of its previous value, and so there is, and indeed never was, a problem. Recent interstellar abundance determinations using observations of solar-type F and G stars in the galactic neighborhood (Jensen et al., 2005; Sofia and Meyer, 2001) suggest that many elemental abundances in the ISM are close to solar abundances and that the observed deviations are random (Jenkins, 2009). However, and as Jenkins (2009) has shown, there still remains an 'oxygen problem' because its differential depletion is barely consistent with its incorporation into oxides and silicates at low depletions but that at high depletions the loss of oxygen from the gas cannot be accounted for by its incorporation into only oxides and silicates. This suggests that the 'missing' oxygen is bound into a phase with hydrogen and carbon atoms that does not contain nitrogen (Jenkins, 2009) and that it could be some form of 'organic refractory' material (Whittet, 2010). However, and for the moment, the 'missing' oxygen problem remains an unsolved mystery.

2.2.3 Summary

Updated solar photospheric abundances are compared with meteoritic abundances. The uncertainties of solar abundances of many trace elements are considerably reduced compared to the 2003 compilation. Some of the solar photosphere REE abundances have now assigned errors of ±5%, approaching the accuracy of meteorite analyses. The agreement between photospheric abundances and CI chondrites is further improved. Problematic elements with comparatively large differences between solar and meteoritic abundances are manganese, hafnium, rubidium, gallium, and tungsten. The CI chondrites match solar abundances in refractory lithophile, siderophile, and volatile elements. All other chondrite groups differ from CI chondrites. With analytical uncertainties, there are no obvious fractionations between CI chondrites and solar abundances.

Further progress will primarily come from improved solar abundance determinations. The limiting factor in the accuracy of meteorite abundances is the inherent variability of CI chondrites, primarily the Orgueil meteorite.

The ISM from which the solar system formed has volatile and moderately volatile element abundances within a factor of 2 of those in the Sun. The more refractory elements of the ISM are depleted from the gas and are concentrated in grains.

References

Allende Prieto C, Lambert DL, and Asplund M (2001) The forbidden abundance of oxygen in the Sun. *The Astrophysical Journal* 556: L63–L66.

Anders E and Grevesse N (1989) Abundances of the elements: Meteoritic and solar. *Geochimica et Cosmochimica Acta* 53: 197–214.

Anders E and Zinner E (1993) Interstellar grains in primitive meteorites: Diamond, silicon carbide, and graphite. *Meteoritics* 28: 490–514.

Armytage RMG, Georg RB, Savage PS, Williams HM, and Halliday AN (2011) Silicon isotopes in meteorites and planetary core formation. *Geochimica et Cosmochimica Acta* 75: 3662–3676.

Arndt P, Bohsung J, Maetz M, and Jessberger E (1996) The elemental abundances in interplanetary dust particles. *Meteoritics and Planetary Science* 31: 817–833.

Asplund M, Grevesse N, Sauval J, and Scott P (2009) The chemical composition of the Sun. *Annual Review of Astronomy and Astrophysics* 47: 481–522.

Babechuk MG, Kamber BS, Greig A, Canil D, and Kodolányi J (2010) The behaviour of tungsten during mantle melting revisited with implications for planetary differentiation time scales. *Geochimica et Cosmochimica Acta* 74: 1448–1470.

Baker RGA, Schönbächler M, Rehkämper M, Williams HM, and Halliday AN (2010) The thallium isotope composition of carbonaceous chondrites – New evidence for live ^{205}Pb in the early solar system. *Earth and Planetary Science Letters* 291: 39–47.

Barrat JA, Zanda B, Moynier F, Bollinger C, Liorzou C, and Bayon G (2012) Geochemistry of CI chondrites revisited: Major and trace elements, and Cu and Zn isotopes. *Geochimica et Cosmochimica Acta* 83: 79–92.

Beer H, Walter G, Macklin RL, and Patchett PJ (1984) Neutron capture cross sections and solar abundances of ^{160,161}Dy, ^{170,171}Yb, ^{175,176}Lu, and ^{176,177}Hf for the *s*-process analysis of the radionuclide ^{176}Lu. *Physical Review C* 30: 464–478.

Begemann F (1980) Isotope anomalies in meteorites. *Reports on Progress in Physics* 43: 1309–1356.

Bischoff A, Palme H, Ash RD, et al. (1993) Paired Renazzo-type (CR) carbonaceous chondrites from the Sahara. *Geochimica et Cosmochimica Acta* 57: 1587–1603.

Blackwell-Whitehead R, Pavlenko YV, Nave G, et al. (2011) Infrared Mn I laboratory oscillator strengths for the study of late type stars and ultracool dwarfs. *Astronomy and Astrophysics* 525: A44.

Bouvier A, Vervoort JD, and Patchett PJ (2008) The Lu-Hf and Sm-Nd isotopic composition of CHUR: Constraints from unequilibrated chondrites and implications for the bulk composition of terrestrial planets. *Earth and Planetary Science Letters* 273: 48–57.

Burnett DS and Woolum DS (1990) The interpretation of solar abundances at the N=50 neutron shell. *Astronomy and Astrophysics* 228: 253–259.

Caffau E, Ludwig H-G, Bonifacio P, et al. (2010) The solar photospheric abundance of carbon. Analysis of atomic carbon lines with the CO5BOLD solar model. *Astronomy and Astrophysics* 514: A92.

Caffau E, Ludwig H-G, Steffe M, Freytag B, and Bonifacio P (2011a) Solar chemical abundances determined with a CO5BOLD 3D model atmosphere. *Solar Physics* 268: 255–269.

Caffau E, Faraggiana R, Ludwig H-G, Bonifacio P, and Steffen M (2011b) The solar photospheric abundance of zirconium. *Astronomische Nachrichten* 332: 128–139.

Caffau E, Ludwig HG, Steffen M, et al. (2008) The photospheric solar oxygen project. I. Abundance analysis of atomic lines and influence of atmospheric models. *Astronomy and Astrophysics* 488: 1031–1046.

Caffau E, Maiorca E, Bonifacio P, et al. (2009) The solar photospheric nitrogen abundance. Analysis of atomic transitions with 3D and 1D model atmospheres. *Astronomy and Astrophysics* 498: 877–884.

Cameron AGW (1973) Abundances of the elements in the Solar System. *Space Science Reviews* 15: 121–146.

Cartledge SIB, Meyer DM, and Lauroesch JT (2001) Space telescope imaging spectrograph observations on interstellar oxygen and krypton in translucent clouds. *The Astrophysical Journal* 562: 394–399.

Clayton RN (1993) Oxygen isotopes in meteorites. *Annual Review of Earth and Planetary Sciences* 21: 115–149.

Clayton RN (2002) Self-shielding in the solar nebula. *Nature* 415: 860–861.

Cowley CR (1995) *An Introduction to Cosmochemistry*, 480 p. Cambridge: Cambridge University Press.

Dauphas N, Remusat L, Chen JH, et al. (2010) Neutron-rich chromium isotope anomalies in supernova nanoparticles. *The Astrophysical Journal* 720: 1577–1591.

Dodd RT (1981) *Meteorites: A Petrologic-Chemical Synthesis*, 368 pp. Cambridge: Cambridge University Press.

Fischer-Gödde M, Becker H, and Wombacher F (2010) Rhodium, gold and other highly siderophile element abundances in chondritic meteorites. *Geochimica et Cosmochimica Acta* 74: 356–379.

Flynn GJ, Bajt S, Sutton S, Zolensky ME, Thomas KL, and Keller LP (1996) The abundance pattern of elements having low nebular condensation temperatures in interplanetary dust particles: Evidence for a new chemical type of chondritic material. In: Gustafson AS and Hanner MS (eds.) *Physics, Chemistry, and Dynamics of Interplanetary Dust*. *ASP Conference Series,* Vol. 104, pp. 291–2204. San Francisco: Astronomical Society of Pacific.

Goldschmidt VM (1938) Geochemische Verteilungsgestze der Elemente IX. Die Mengenverhätnisse der Elemente und der Atom-Arten. *Skrifter Utgitt av Det Norske Vidensk. Akad. Skrifter I. Mat. Naturv* 148, Kl. No. 4, 1–148.

Grevesse N and Sauval AJ (1998) Standard solar composition. *Space Science Reviews* 85: 161–174.

Grossman L and Larimer JW (1974) Early chemical history of the solar system. *Reviews of Geophysics and Space Physics* 12: 71–101.

Harkins WD (1917) The evolution of the elements and the stability of complex atoms. *Journal of the American Chemical Society* 39: 856–879.

Hidaka H and Yoneda S (2011) Diverse nucleosynthetic components in barium isotopes of carbonaceous chondrites: Incomplete mixing of *s*- and *r*-process isotopes and extinct ^{135}Cs in the early solar system. *Geochimica et Cosmochimica Acta* 75: 3687–3697.

Holweger H (2001) Photospheric abundances: Problems, updates, implications. In: Wimmer-Schweinsgruber RF (ed.) *Solar and Galactic Composition*, pp. 23–30. Melville, NY: American Institute of Physics.

Horan MF, Walker RJ, Morgan JW, Grossman JN, and Rubin AE (2003) Highly siderophile elements in chondrites. *Chemical Geology* 196: 5–20.

Howk C, Savage BD, and Fabian D (1999) Abundances and physical conditions in the warm neutral medium toward μ Columbae. *The Astrophysical Journal* 525: 253–293.

Hyman M and Rowe MW (1983) Magnetite in CI chondrites. *Journal of Geophysical Research* 88: A736–A740.

Jenkins EB (2009) A unified representation of gas-phase element depletions in the interstellar medium. *The Astrophysical Journal* 700: 1299–1348.

Jensen AG, Rachford BL, and Snow TP (2005) Abundances and depletions of interstellar oxygen. *The Astrophysical Journal* 619: 891–913.

Jessberger EK, Christoforidis A, and Kissel J (1988) Aspects of the major element composition of Halley's dust. *Nature* 332: 691–695.

Jones AP (2000) Depletion patterns and dust evolution in the interstellar medium. *Journal of Geophysical Research* 105: 10257–10268.

Kleine T, Mezger K, Münker C, Palme H, and Bischoff A (2004) ^{182}Hf–^{182}W isotope systematics of chondrites, eucrites, and Martian meteorites: Chronology of core formation and mantle differentiation in Vesta and Mars. *Geochimica et Cosmochimica Acta* 68: 2935–2946.

Lodders K (2003) Solar system abundances and condensation temperatures of the elements. *The Astrophysical Journal* 591: 1220–1247.

Lodders K and Amari S (2005) Presolar grains from meteorites: Remnants from the early times of the solar system. *Chemie Der Erde* 65: 93–166.

Lodders K and Fegley B Jr. (2011) *Chemistry of the Solar System*, 476 p. Cambridge: RSC Publishing, Royal Society of Chemistry.

Lodders K and Osborne R (1999) Perspectives on the comet-asteroid-meteorite link. *Space Science Reviews* 90: 289–297.

Lodders K, Palme H, and Gail HP (2009) Abundances of the elements in the solar system. In: Trümper JE (ed.) *Landolt-Börnstein*, New Series, VI/4B, pp. 560–598. Berlin: Springer.

Lu Y, Makishima A, and Nakamura E (2007) Coprecipitation of Ti, Mo, Sn and Sb with fluorides and application to determination of B, Ti, Zr, Nb, Mo, Sn, Sb, Hf and Ta by ICP-MS. *Chemical Geology* 236: 13–26.

Ludwig HG and Steffen M (2008) Precision spectroscopy in astrophysics. In: Santos NC, Pasquini L, Correia ACM, and Romanielleo M (eds.) *Proceedings of the ESO/Lisbon/Aveiro Conference Held in Aveiro, Portugal, 11–15 September 2006*, Garching, Germany, 133–138.

Makishima A and Nakamura E (2006) Determination of major, minor and trace elements in silicate samples by ICP-QMS and ICP-SF-MS applying isotope dilution-internal standardisation (ID-IS) and multi-stage internal standardisation. *Geostandards and Geoanalytical Research* 30: 245–271.

Marty B, Chaussidon M, Wiens RC, Jurewicz AJG, and Burnett DS (2011) A ^{15}N-poor isotopic composition for the solar system as shown by Genesis solar wind samples. *Science* 332: 1533–1536.

Mashonkina L, Gehren T, Shi JR, Korn AJ, and Grupp F (2011) A non-LTE study of neutral and singly-ionized iron line spectra in 1D models of the Sun and selected late-type stars. *Astronomy and Astrophysics* 528: A87.

Mathis JS (1990) Interstellar dust and extinction. *Annual Review of Astronomy and Astrophysics* 28: 37–70.

McKeegan KD, Kallio APA, Heber VS, et al. (2011) The oxygen isotopic composition of the Sun inferred from captured solar wind. *Science* 332: 1528–1532.

Melendez J and Asplund M (2008) Another forbidden solar oxygen abundance: The [O I] 5577 Å line. *Astronomy and Astrophysics* 490: 817–821.

Melendez J and Barbuy B (2009) Both accurate and precise gf-values for Fe II lines. *Astronomy and Astrophysics* 497: 611–617.

Meyer DM, Jura M, and Cardelli JA (1998) The definitive abundance of interstellar oxygen. *Astrophysical Journal* 493: 222–229.

Morlok A, Bischoff A, Stephan T, Floss C, Zinner E, and Jessberger EK (2006) Brecciation and chemical heterogeneities of CI chondrites. *Geochimica et Cosmochimica Acta* 70: 5371–5394.

Morton DC and Spitzer L (1966) Line spectra of delta and pi Scorpii in the far-ultraviolet. *The Astrophysical Journal* 144: 1–12.

Münker C, Pfänder JA, Weyer S, Büchl A, Kleine T, and Mezger K (2003) Evolution of planetary cores and the Earth-Moon system from Nb/Ta systematics. *Science* 301: 84–87.

Nilsson H, Hartman H, Engström L, et al. (2010) Transition probabilities of astrophysical interest in the niobium ions Nb^{+} and Nb^{2+}. *Astronomy and Astrophysics* 511: A16.

Pack A, Russell SS, Shelley JMG, and van Zuilen M (2007) Geo- and cosmochemistry of the twin elements yttrium and holmium. *Geochimica et Cosmochimica Acta* 71: 4592–4608.

Palme H (2000) Are there chemical gradients in the inner solar system?. *Space Science Reviews* 92: 237–264.

Palme H and Beer H (1993) Abundances of the elements in the solar system. In: Voigt HH (ed.) *Landolt-Börnstein, Group VI: Astronomy and Astrophysics*, Vol. 3a: *Instruments; Methods; Solar System,* pp. 196–221. Berlin: Springer.

Palme H, Larimer JW, and Lipschutz ME (1988) Moderately volatile elements. In: Kerridge JF and Matthews MS (eds.) *Meteorites and the Early Solar System*, pp. 436–461. Tucson: University of Arizona Press.

Palme H and Lodders K (2009) Metal-silicate fractionation in carbonaceous chondrites. *Meteoritics and Planetary Science* 44: A165.

Patzer A, Pack A, and Gerdes A (2010) Zirconium and hafnium in meteorites. *Meteoritics and Planetary Science* 45: 1136–1151.

Petaev M and Wood JA (1998) The condensation with partial isolation model of condensation in the solar nebula. *Meteoritics and Planetary Science* 33: 1123–1137.

Piersanti L, Straniero O, and Cristallo S (2007) A method to derive the absolute composition of the solar system, and the stars. *Astronomy and Astrophysics* 462: 1061–1062.

Pourmand A, Dauphas N, and Ireland TJ (2012) A novel extraction chromatography and MC-ICP-MS technique for rapid analysis of REE, Sc and Y: Revising CI-chondrite abundances. *Chemical Geology* 291: 38–54.

Qin L, Nittler LR, Alexander CMO'D, Wang J, Stadermann FJ, and Carlson RW (2011) Extreme ^{54}Cr-rich nano-oxides in the CI chondrite Orgueil – Implication for a late supernova injection into the solar system. *Geochimica et Cosmochimica Acta* 75: 629–644.

Rammensee W and Palme H (1982) Metal-silicate extraction technique for the analysis of geological and meteoritic samples. *Journal of Radioanalytical Chemistry* 71: 401–418.

Russell NH (1929) The composition of the Sun's atmosphere. *The Astrophysical Journal* 70: 11–82.

Savage BD and Sembach KR (1996) Interstellar abundances from absorption-line observations with the Hubble Space Telescope. *Annual Review of Astronomy and Astrophysics* 34: 279–329.

Schulze H, Kissel J, and Jessberger EK (1997) Chemistry and mineralogy of Comet Halley's Dust. In: Pendleton YJ and Tielens AGGM (eds.) *From Stardust to Planetesimals*. *ASP Conference Series*, Vol. 122, pp. 397–414. San Francisco: Astronomical Society of the Pacific.

Sneden C, Lawler JE, Cowan JJ, Ivans II, and Den Hartog EA (2009) New rare earth element abundance distributions for the Sun and five *r*-process-rich very metal-poor stars. *Astrophysical Journal Supplement* 182: 80–96.

Snow TP (2000) Composition of interstellar gas and dust. *Journal of Geophysical Research* 105: 10239–10248.

Snow TP, Destree JD, and Jensen AG (2007) The abundance of interstellar fluorine and its implications. *The Astrophysical Journal* 655: 285–298.

Snow TP and Witt AN (1996) Interstellar depletions updated: Where all the atoms went. *The Astrophysical Journal* 468: L65–L68.

Sofia UJ and Meyer DM (2001) Interstellar abundance standards revisited. *The Astrophysical Journal* 554: L221–L224.

Sofia UJ, Meyer DM, and Cardelli JA (1999) The abundance of interstellar tin and cadmium. *The Astrophysical Journal* 522: L137–L140.

Sofia UJ, Parvathi VS, Babu BRS, and Murthy J (2011) Determining interstellar carbon abundances from strong-line transitions. *The Astronomical Journal* 141: 22–27.

Suess H (1947) Über kosmische Kernhäufigkeiten I. Mitteilung: Einige Häufigkeitsregeln und ihre Anwendung bei der Abschätzung der Häufigskeitwerte für die mittelsschweren und schweren Elemente. II. Mitteilung: Einzelheiten in der Häufigskeitverteilung der mittelschweren und schweren Kerne. *Zeitschrift für Naturforschung* 2a(311–321): 604–608.

Suess HE and Urey HC (1956) Abundances of the elements. *Reviews of Modern Physics* 28: 53–74.

Suess HE and Zeh HD (1973) The abundances of the heavy elements. *Astrophysics and Space Science* 23: 173–187.

Wai CM and Wasson JT (1977) Nebular condensation of moderately volatile elements and their abundances in ordinary chondrites. *Earth and Planetary Science Letters* 36: 1–13.

Walker RJ, Horan MF, Morgan JW, Becker H, Grossman JN, and Rubin A (2002) Comparative ^{187}Re–^{187}Os systematics of chondrites: Implications regarding early solar system processes. *Geochimica et Cosmochimica Acta* 66: 4187–4201.

Warren PH (2011) Stable-isotopic anomalies and the accretionary assemblage of the Earth and Mars: A subordinate role for carbonaceous chondrites. *Earth and Planetary Science Letters* 311: 93–100.

Wasson JT (1985) *Meteorites: Their Record of Early Solar-System History*, 267 p. New York: W. H. Freeman.

Whittet DCB (2010) Oxygen depletion in the interstellar medium: Implications for grain models and the distribution of elemental oxygen. *The Astrophysical Journal* 710: 1009–1016.

Wolf D and Palme H (2001) The solar system abundances of P and Ti and the nebular volatility of P. *Meteoritics and Planetary Science* 36: 559–572.

Yin Q, Jacobsen SB, Yamashita K, Blichert-Toft J, Télouk P, and Albarède F (2002) A short timescale for terrestrial planet formation from Hf–W chronometry of meteorites. *Nature* 418: 949–952.